ISSN: 2634-9221
European Journal of Applied Sciences; Vol. 14 No. 02 (2026) (460-492)
https://doi.org/10.14738/aivp.1402.20058

Epidermal Growth Factor Network Modulation of Immature Central Nervous System Neuronal Functions and the Inhibitory Effects of Ethanol: Relevance to Fetal Alcohol Spectrum Disorder

Ming Tong[1] and Suzanne M. de la Monte[2]

1. Department of Medicine, Rhode Island Hospital, Brown University Health, Alpert Medical School of Brown University, Providence, RI USA
2. Departments of Pathology and Laboratory Medicine, Neurology, Neurosurgery, and Medicine, Rhode Island Hospital, Brown University Health, Alpert Medical School of Brown University, Providence, RI USA

Abstract: This study characterizes the effects of epidermal growth factor receptor (EGFR) modulation of growth, metabolic activity, and aspartyl-asparaginyl-β-hydroxylase (ASPH) expression in immature central nervous system neuronal cells (PNET2), crosstalk with insulin/insulin-like growth factor (IGF)/insulin receptor substrate (IRS) and Notch networks, and the effects of ethanol exposure on EGFR-regulated responses. Validation studies were conducted with cerebellar tissue and slice cultures from a fetal alcohol spectrum disorder rat model. PNET2 cell growth, viability, metabolic function, and ASPH expression were supported by EGF, TGF-α, and TGF-β. Those effects were associated with increased tyrosine phosphorylation of EGFR. TGF-β exhibited stimulatory crosstalk with the IGF1 pathway and Notch transcription factors, whereas EGF and TGF-α had inhibitory effects on INSULIN and IGF1 receptor and IRS1 mRNA. Ethanol exposure significantly inhibited EGF, TGF-α, and TGF-β-stimulated pY-EGFR, PCNA, and ASPH expression in PNET2 and rat cerebellar slice cultures. The findings herein establish that EGFR pathways regulate critical functions in immature CNS neuronal cells, including ASPH, which mediates cell migration during development. Crosstalk between EGF or TGF-α and insulin/IGF networks was largely inhibitory, whereas between TGF-β and insulin/IGF or Notch networks, the crosstalk was stimulatory. Ethanol's prominent inhibitory effects on EGFR networks and activation of ASPH likely contribute to the FASD-associated impairments in cerebellar development and function. Therapeutic measures that fortify EGFR signaling through Notch and ASPH may reduce the adverse effects of prenatal alcohol exposure on the brain.

Keywords: fetal alcohol spectrum disorder, epidermal growth factor, notch, cerebellum, aspartyl-asparaginyl-β-hydroxylase, Transforming growth factor, neuronal migration

INTRODUCTION

Prenatal alcohol exposures cause characteristic craniofacial dysmorphic features together with sustained structural and functional brain pathologies linked to neurocognitive and neurobehavioral deficits. These adverse effects of alcohol are collectively termed fetal alcohol spectrum disorder (FASD) [1-4]. Binge or chronic alcohol exposures during development cause FASD, but the severity of abnormalities is dose-, duration-, and timing-dependent [5, 6]. The cerebellum is one of the major targets of alcohol-related brain damage [2, 7]. In addition to its toxic and degenerative effects on growth and survival, ethanol impairs neuronal migration, plasticity, circuitry, and metabolism, which are broadly needed to support neurodevelopmental functions [8-11] including plasticity [12]. Prenatal

alcohol exposure also compromises the viability and function of glia [13-15], particularly oligodendrocytes [16], which are required for myelin formation. Subsequent reductions in the integrity and abundance of mature myelin mediate white matter hypotrophy [15, 17, 18] and contribute to cognitive and motor deficits in FASD due to compromised speed of conductivity, and loss of axonal and dendritic inter-neuronal connections [15, 17, 18].

Previous studies have demonstrated the importance of insulin and insulin-like growth factor (IGF) signaling in neurodevelopment, and that major adverse effects of prenatal alcohol exposure include impairments in insulin and IGF signaling [19-21]. Insulin and IGF mediate broad functions in the brain, supporting neuronal growth, survival, plasticity, energy metabolism, and migration [22, 23]. These effects are mediated by downstream signaling via PI3K-Akt and mTOR [23]. Ethanol's inhibitory effects on insulin- and IGF-regulated functions in the immature brain have been linked to impairments in signaling at multiple levels of the cascade, beginning with receptor tyrosine phosphorylation and extending downstream through insulin receptor substrate, PI3K, and Akt [22, 23]. In addition to inhibiting Akt, GSK-3β is activated by various mechanisms, including inhibition of PI3K, increased oxidative stress, and increased activity of phosphatases, resulting in dephosphorylation and activation of GSK-3β. Further studies demonstrated that long-term effects of prenatal alcohol exposure include inhibition of signaling through mTOR, which also has diverse roles in regulating neuronal metabolic functions [24, 25].

An important downstream target of insulin/IGF signaling that is inhibited by prenatal alcohol exposure is aspartyl-asparginyl-β-hydroxylase (ASPH) [26-30]. ASPH is a critical regulator of immature cell growth and migration [31-34]. Ethanol-mediated inhibition of ASPH causes dose-dependent impairments in cerebellar neuron migration [28] and is linked to motor dysfunction [35]. ASPH is regulated at the mRNA and protein levels [36]. ASPH protein expression can be reduced via declines in mRNA transcript abundance or increased proteolytic degradation [26, 28]. Ethanol's inhibitory effects on ASPH are linked to impaired signaling through insulin/IGF-IRS-Akt-mTOR (mechanistic target of rapamycin) networks [23]. ASPH functions by interacting with and hydroxylating epidermal growth factor (EGF)-like domains expressed in key signaling molecules in the Notch pathway, including Notch and Jagged [36-39]. ASPH's catalytic activity drives Notch signaling and promotes cell motility [31, 36]. This pathway and mechanism have been demonstrated to be functional both in development [35] and various malignancies [31, 40, 41] and inhibited by ethanol [29].

Epidermal growth factor signaling regulates growth, survival, proliferation, and differentiation in various cell types. EGF signaling is activated through the binding of trophic factor ligands and tyrosine phosphorylation of the EGF receptor (EGFR). EGF, a 53 amino acid peptide, is one of the main activators of EGFR signaling. Transforming growth factor-alpha (TGF-α) and TGF-β are additional key trophic factors that regulate EGFR signaling networks. Both EGF and TGF-α activate Ras/MAPK, PI3K/Akt, mTOR, and JAK/STAT, promoting cell proliferation, differentiation, and survival [42-44]. TGF-β functions by indirectly transactivating the EGFR, promoting cell migration and invasion [45, 46]. EGFR signaling likely plays important roles in neurodevelopment, particularly in the cerebellum, based on expression patterns [47]. Therefore, crosstalk between insulin/IGF and EGF pathways is an important consideration for brain development.

Publications on prenatal alcohol exposure effects on EGFR signaling in the brain are relatively scant. However, exploratory studies suggested that ethanol inhibits EGFR signaling in the CNS. Although it is known that ASPH functions by interacting with EGF-like domains to trigger signal transduction cascades involving Notch [31, 36, 39, 48], its effects on EGFR pathways have not been studied. It is noteworthy that many malignancies with prominently activated EGFR signaling overexpress ASPH [41, 49-51]. Therefore, it is hypothesized that developmental ethanol exposure inhibits CNS EGFR signaling networks by reducing trophic factor-mediated tyrosine phosphorylation of the EGFR. Attenuation of downstream pathways reduces ASPH expression and Notch activation. Ethanol's inhibitory effects on EGFR could be mediated by reduced kinase or increased phosphatase activation, and/or reduced EGFR expression, all of which have been demonstrated for insulin and IGF-1 signaling in FASD models [26, 28, 52, 53].

Since the published literature on neuronal EGFR signaling during development was extremely scant, the first objective of this study was to characterize the effects of EGF, TGF-α, and TGF-ß stimulation on growth, metabolic activity, EGFR signaling, and ASPH expression in human immature CNS neuronal cells of cerebellar origin (PNET2 cells). The second goal was to examine crosstalk between EGFR-activated signaling and insulin/IGF and Notch pathways. The third objective was to examine the effects of ethanol exposure on EGFR signaling in PNET2 cells and to validate these findings using in vivo and ex vivo experimental models of FASD.

METHODS

Growth Factor Stimulation Studies

Human PNET2 CNS-derived cerebellar neuronal cells [54] were maintained in antibiotic-free Dulbecco's modified Eagle's Medium (DMEM) supplemented with 5% fetal bovine serum (FBS), 4mM glutamine, and 4.5g/L glucose, and in a standard 5% CO_2 incubator.

To study the effects of growth factor stimulation on cell growth, metabolic activity, and viability, freshly seeded subconfluent 96-well cultures containing 4000 viable (Trypan blue-excluded) cells per well in 100µL of culture medium were serum-deprived overnight, then stimulated for 24 hours with 1-10% FBS, or 1-10 ng/mL EGF, IGF-1, TGF-α, or TGF-ß (Supplementary Table 1; Table S1). To further examine the role of EGF pathway signaling in relation to cell growth and viability, PNET2 96-well cultures were treated with a dose range of EGFR (AG1478 and GEFINTIB) or Notch (ZLDI-8-ADAM17 and GI 254023X/ADAM10) inhibitors for 24 hours (Table S1). The treated cultures were assayed for metabolic activity and viability.

Table 1: ANOVA – AUC Results for PNET2 Cell Trophic Factor Stimulation

Index	F-Ratio	p-Value
MTT	56.25	0.001
H33342	306.9	<0.0001
MTT/H33342	129.3	0.0002

Table S1: Trophic Factors and Inhibitors

Compound	Source	Company Location	Catalogue#	Concentration
Insulin Novolin-R	Novo Nordisk Pharmaceutical	Bagsvaerd, Denmark	U 100, NDC 0169-1833-11	0.1-1.0 IU/mL
IGF-1	MilliporeSigma	St. Louis, MO USA	I3769	10 ng/mL
EGF	MilliporeSigma	St. Louis, MO USA	SRP3027	10 or 20 ng/mL
TGF-α	Abcam	Cambridge, MA USA	ab283419	20 or 20 ng/mL
TGF-ß	Abcam	Cambridge, MA USA	ab50036	10 or 20 ng/mL
AG-1478	Selleckchem	Houston, TX USA	S2728	3.125-100 µM
Gefitinib	Selleckchem	Houston, TX USA	S1025	0.0625-2 µM
ZLDI-8	MedChemExpress	Monmouth Junction, NJ USA	HY-123931	3.125-100 µM
GI254023X	MedChemExpress	Monmouth Junction, NJ USA	HY-19956	0.625-20 µM

Trophic factors and inhibitor compounds used in cell culture. IGF-1=insulin like growth factory, type 1; EGF= epidermal growth factor; TGF-α = transforming growth factor-alpha; TGF-ß = transforming growth factor-beta; AG-1478 and Gefitinib = EGFR inhibitors; ZLDI-8 and GI254023X = Notch inhibitors.

Materials

Critical chemicals and reagents are listed in Table S2. All other fine reagents were purchased from CalBiochem/Millipore Sigma (Burlington, MA, USA), Pierce Chemical (Dallas, TX, USA), or MilliporeSigma (St. Louis, MO, USA).

Table S2: Critical Reagents

Material/Reagent/Equipment	Source	Company Location
Materials and Instruments		
Modular Incubator Chamber	Embrient, Inc.	San Diego, CA USA
Shandon Cytospin 3	Marshall Scientific,	Hampton, NH, USA
Spectra-Max M5 Multimode Plate Reader	Molecular Devices	Sunnyvale, CA, USA
MaxiSorp 96-well plates	Thermo-Fisher Scientific	Bedford, MA USA
Luminex MAGPIX Instrument	Diasorin	Austin, TX USA
Cellular and Immunoassay Reagents		
3-(4,5-dimethylthiazol-2-yl)-2,5-diphenyltetrazolium bromide (MTT) (#M5655)	MilliporeSigma	St. Louis, MO, USA
Hoechst 33342 (H3570)	MilliporeSigma	St. Louis, MO, USA
Crystal Violet	Thermo Scientific Chemicals	Haverhill, MA, USA)
Cytoseal 60 Mounting Medium	Epredia Inc	Portsmouth, NH USA
Bicinchoninic Acid Assay Reagents	Thermo-Fisher Scientific	Bedford, MA USA
Superblock TBS	Thermo-Fisher Scientific	Bedford, MA USA
Proton Biotin Protein Labeling Kit	Vector Laboratories	Newark, CA, USA
Horseradish peroxidase-conjugated secondary antibodies	Thermo-Fisher Scientific	Bedford, MA USA
Amplex UltraRed Soluble Fluorophore	Life Technologies	Carlsbad, CA, USA
Alkaline phosphatase streptavidin	Vector Laboratories	Newark, CA, USA
4-Methylumbelliferyl phosphate	Life Technologies	Carlsbad, CA, USA
ImmPRESS Peroxidase Polymer Detection Reagents	Vector Laboratories	Newark, CA, USA
Streptavidin Cyanine5 (Cy5) Dye	Thermo-Fisher Scientific	Bedford, MA USA
Commercial Kits and Reagents for Multiplex Assays		
Qiazol Lysis Reagent	Qiagen	Germantown, MD USA
Quantigene Plex Panels	Invitrogen-Thermo-Fisher Scientific	Bedford, MA USA
xMAP Reagents	MilliporeSigma	St. Louis, MO, USA

Cellular Metabolic Activity and Viability

The 3-(4,5-dimethylthiazol-2-yl)-2,5-diphenyltetrazolium bromide (MTT) (#M5655, MilliporeSigma, St. Louis, MO, USA) assay for measuring metabolic function was performed

in 96-well cultures (100 µL) by adding 10µL/well of freshly prepared MTT solution (5 mg/mL in MEM without phenol red). After 20 minutes of incubation at 37°C in a 5% CO_2 atmosphere, the culture medium was replaced with 100µL of acidic isopropanol (0.04 mol/L HCl/isopropanol) to elute the reaction product (5 minutes incubation at room temperature). The absorbances were measured at 540nm in a Spectra-Max M5 Multimode Plate Reader (Molecular Devices, Sunnyvale, CA, USA). Hoechst dye staining measured cell number (growth) in the same wells as the MTT assay, enabling calculation of metabolic function adjusted for cell number. For this assay, the MTT eluate buffer was replaced with 50µL of 10µg/mL Hoechst 33342 dye (H3570, Invitrogen, fluorescence Carlsbad, CA, USA) in phosphate-buffered saline (PBS). After 5 minutes of room-temperature incubation with light shielding, fluorescence intensity (Ex 360 nm/Em 460 nm) was measured in a Spectra-Max M5 Multimode Plate Reader (Molecular Devices, Sunnyvale, CA, USA).

Parallel cultures were identically treated and assayed for cell viability by crystal violet staining as previously described [55]. In brief, after removing the culture medium and rinsing with PBS, the cells were stained with 50µL of Crystal Violet (Thermo Scientific Chemicals, Haverhill, MA, USA) solution (0.5% crystal violet in 100 mL 20% methanol) for 10 minutes at room temperature. After removing excess crystal violet by thorough washing in distilled water, the plates were air-dried, and the cellular Crystal violet dye was eluted with 200µL methanol. Absorbances were measured at 570 nm in a Spectra-Max M5 Multimode Plate Reader (Molecular Devices, Sunnyvale, CA, USA).

Cellular Morphology

Cytospin preparations of PNET2 cells were used for cytomorphological studies. Cultured cells were detached, dissociated with trypsin-EDTA, pelleted, and re-suspended in culture medium containing 0.5% FBS to prevent non-specific lysis. Approximately $0.5x10^5$ viable cells were centrifuged onto Plus-charged glass microscope slides at 600 rpm for 5 minutes at room temperature, using a Shandon Cytospin 3 Cytology Centrifuge (Marshall Scientific, Hampton, NH, USA). The slides were immediately submerged in 10% neutral-buffered formalin for cell fixation. After staining with Crystal violet, the cells were rapidly dehydrated through graded ethanol solutions and preserved under coverglass with Cytoseal 60 mounting media (Epredia; REF# 8310-4) for light microscopic examination.

Immunoassays of Protein Expression

To measure immunoreactivity by duplex ELISA, the cultured cells were homogenized in weak lysis buffer (50 mM Tris (pH 7.5), 150 mM NaCl, 5 mM EDTA (pH 8.0), 50 mM NaF, 0.1% Triton X-100) containing protease inhibitor cocktail (1mM PMSF, 0.1 mM TPCK, 2 µg/ml aprotinin, 2 µg/ml pepstatin A, 1 µg/ml leupeptin) and a phosphatase inhibitor [sodium vanadate]. The homogenates were centrifuged at 14,000 rpm for 10 minutes at 4°C to obtain clarified supernatants, which were used in protein assays. Protein concentration was measured with the bicinchoninic acid (BCA) assay.

The antibodies used in these assays are listed in Table S3. For the direct binding ELISAs, samples containing 50ng protein in 50µL of bicarbonate-binding buffer were distributed into 96-well MaxiSorp plates for overnight adsorption at 4°C. Superblock TBS was used to mask non-specific binding sites. Sequential incubations with primary antibodies (0.2-

5.0 µg/ml; overnight at 4°C), horseradish peroxidase-conjugated secondary antibody, and Amplex UltraRed soluble fluorophore were used to detect immunoreactivity, which was measured in a SpectraMax M5 Multimode Plate Reader (Molecular Devices, Sunnyvale, CA, USA) (Ex 530 nm/Em 590 nm). Parallel reactions measured immunoreactivity to large acidic ribosomal protein (RPLPO) as a housekeeping control [56]. All assays were performed in triplicate. The calculated ratios of target to control protein or protein content in the wells were used for inter-group statistical comparisons.

Table S3: Antibodies Used in ELISAs

Antibody Targets*	Source	Concentration	Source	Company Location	Catalogue#	RRID
EGFR (EP38Y)	Mouse	0.208 µg/mL	Abcam	Cambridge, MA USA	ab52894	AB_869579
Phospho-EGF Receptor (Ser1046/1047)	Rabbit	0.016 µg/mL	Cell Signaling Technology	Danvers, MA	#2238	AB_331129
Phospho-EGF Receptor (Tyr1068)	Rabbit	0.6 µg/mL	Invitrogen (Thermo-Fisher Scientific)	Carlsbad, CA USA	44-788G	AB_331792
PCNA	Mouse	0.5 µg/mL	BD Biosciences	Milpitas, CA USA	610664	AB_397991
ASPH-A85G6	Mouse	1.3 µg/mL	Liver Research Center Brown University Health	Providence, RI USA	LRC-A85G6	N/A
ASPH-FB50	Mouse	0.845 µg/mL	Liver Research Center Brown University Health	Providence, RI USA	LRC-FB50	N/A
p44/42 MAPK (Erk1/2)	Rabbit	0.1 µg/mL	Cell Signaling Technology	Danvers, MA	9102	AB_330744
Phospho-p44/42 MAPK (Erk1/2) (Thr202/Tyr204)	Rabbit	0.5 µg/mL	Cell Signaling Technology	Danvers, MA	4370	AB_2315112
RPLPO	Mouse	0.1 µg/mL	Santa Cruz Biotechnology	Dallas, TX USA	sc-293260	AB_628218

*EGFR=epidermal growth factor receptor; pS-EGFR = Serine phosphorylated EGFR; PCNA = proliferating cell nuclear antigen; ASPH-A85G6 = aspartyl-asparaginyl-β-hydroxylase full length protein with catalytic domain; ASPH-FB50 = aspartyl-asparaginyl-β-hydroxylase truncated homolog missing catalytic domain; MAPK = Mitogen-activated protein kinase; RPLPO = large acidic ribosomal protein.

Analysis of mRNA Expression

A custom Quantigene 2.0 multiplex panel (Cat# 312185) measured mRNA transcript abundance corresponding to insulin/IGF and Notch pathway molecules (Table S4) with Hypoxanthine phosphoribosyltransferase 1 (HPRT1) included as the internal control. Total RNA was isolated from PNET2 cells using QIAzol Lysis Reagent (Qiagen, Germantown, MD USA). For the multiplex assays, xMAP fluorescent capture beads suspended in lysis buffer containing blocking reagent and RNA probe sets (pre-amplifier, amplifier, and biotin-label) were dispensed into 96-well plates and incubated overnight with 1µg of total RNA. Then, after incubating the samples with streptavidin-conjugated R-Phycoerythrin, fluorescent signals were quantified in a Luminex MAGPIX instrument (Diasorin, Austin, TX, USA) along with MAGPIX calibration and verification standards to ensure that the fluorescence signals were proportional to RNA transcript abundance captured by the beads. The net results after subtracting probe-related background from the target median fluorescence intensity were normalized to HPRT1 for intergroup statistical comparisons.

Table S4: QuantiGene 2.0 Plex

Bead Number	Gene Symbol	Target Genes
		Insulin/IGF/IRS Network Genes
20	*INS*	*INSULIN*
46	*IGF1*	*INSULIN-LIKE GROWTH FACTOR 1* (somatomedin C)
14	*IGF2*	*INSULIN-LIKE GROWTH FACTOR 2* (somatomedin A)
28	*INSR*	*INSULIN RECEPTOR*
21	*IGF1R*	*INSULIN-LIKE GROWTH FACTOR 1 RECEPTOR*
13	*IGF2R*	*INSULIN-LIKE GROWTH FACTOR 2 RECEPTOR*
30	*IRS1*	*INSULIN RECEPTOR SUBSTRATE 1*
12	*IRS2*	*INSULIN RECEPTOR SUBSTRATE 2*
44	*IRS4*	*INSULIN RECEPTOR SUBSTRATE 4*
		Notch Network Genes
53	*NOTCH1*	*NOTCH HOMOLOG 1*, translocation-associated (Drosophila)
35	*JAG1*	*JAGGED 1* (Alagille syndrome)
33	*ASPH*	*ASPARTATE BETA-HYDROXYLASE*
22	*HES1*	*HAIRY AND ENHANCER OF SPLIT 1*, (Drosophila)
25	*HEY1*	*HAIRY/ENHANCER-OF-SPLIT RELATED WITH YRPW MOTIF 1*
39	*HIF1A*	*HYPOXIA-INDUCIBLE FACTOR 1, ALPHA* subunit (basic helix-loop-helix transcription factor)
		Control Genes
34	*ABCG2*	*ATP-BINDING CASSETTE*, sub-family G (WHITE), member 2
43	*CASR*	*CALCIUM-SENSING RECEPTOR* (hypocalciuric hypercalcemia 1, severe neonatal hyperparathyroidism)
36	*HPRT1*	*HYPOXANTHINE PHOSPHORIBOSYLTRANSFERASE 1*
54	*RPL13A*	*RIBOSOMAL PROTEIN L13A*

In Vitro Ethanol Exposure Model

PNET2 cells were pretreated with 0 mM or 100 mM ethanol in T75 flasks for 72h, with media changed daily to maintain ethanol concentration. For the trophic factor stimulation studies, the cells were reseeded into 12-well plates in medium supplemented with 0.5% FBS and maintained at 37°C in sealed humidified Modular Incubator Chambers (Embrient, Inc, San Diego, CA, USA) in which 0mM or 100mM ethanol was vaporized from a reservoir tray (changed daily). The sealed chambers were equilibrated with gas containing 75% N, 20% O_2, and 5% CO_2. After overnight adaptation to 0.5% FBS containing medium, the cells were stimulated with EGF, TGF-α, TGF-ß, or FBS for 24 hours. At the conclusion of the experiment, the cells were harvested for protein and RNA isolation. Identically treated 6-well cultures were used for cytospin preparations to evaluate the effects of ethanol and trophic factor stimulation of neuronal morphology.

Ex vivo Ethanol Exposure Model

Long Evans rat dams with litters were housed under standardized humane conditions, including a 12-hour light (7AM-7PM)/dark (7PM-7AM) cycle, controlled temperature (70°F-74°F), and free access to food. The Institutional Animal Care and Use Committee (IACUC) at the Lifespan/Rhode Island Hospital approved the use of rats for these experiments. Our approved protocols followed the guidelines established by the National Institutes of Health.

Rat pups were used to generate FASD model for direct studies of cerebellar tissue and to generate ex vivo cerebellar slice cultures for examining the effects of ethanol on EGFR signaling and ASPH expression. The model was generated by binge-administering intraperitoneal injections of saline (vehicle control) or 2g/Kg of ethanol in 50 µL volumes

on postnatal days 4 (P4) and P6 [18]. On P7, the cerebella were harvested and hemi-sected in the mid-sagittal plane. One hemisphere was snap-frozen on dry ice and stored at -80 °C for subsequent studies. The other hemisphere was used for slice cultures [18, 57]. In brief, after chilling in ice-cold Hank's Balanced Salt Solution (HBSS), the cerebella were sliced at 250µm intervals using a McIlwain tissue chopper (Mickle Laboratory Engineering Co. Ltd, UK). The slices were separated under a dissecting microscope and cultured in 12-well Nunc plates (4 or 5 slices per well) that contained 200 µL DMEM supplemented with 10% heat-inactivated FBS, 1X non-essential amino acids solution, 4mM L-glutamine, 4.5g/L glucose, 25mM potassium chloride, 120U/mL Penicillin, 120µg/mL Streptomycin. The cultures were maintained at 37°C in a standard 5% CO_2 incubator. After overnight incubation, the medium was changed, and the cultures were stimulated for 24 h with 0.5% FBS or with 20 ng/mL of EGF, TGF-α, or TGF-β. At the conclusion of the experiment, the slices were harvested in weak lysis buffer containing protease and phosphatase inhibitors (see above). The clarified homogenates were stored at -80°C for immunoreactivity assays.

Data Analysis

The results were analyzed and graphed using GraphPad Prism 10.5 (San Diego, CA, USA). Inter-group comparisons were made with analysis of variance (ANOVA) and post hoc repeated-measures significance tests, or Welch T-tests. Statistical significance was set at $p \leq 0.05$.

RESULTS

EGF Pathway Stimulation of Neuronal Cells (Figure 1)

To examine the effects of EGF pathway stimulation on CNS neuronal metabolic activity and viability, 96-well PNET2 neuronal microcultures were treated with a concentration range of FBS, EGF, TGF-α, TGF-β, or FBS (positive control). The effects of treatment were illustrated graphically and statistically compared using area under the curve analysis and one-way ANOVA (Table 1) with post hoc Tukey's Test (Figure 1). MTT activity increased with the concentration of FBS or trophic factor, but FBS consistently produced sharply higher levels of MTT relative to the specific trophic factors (Figure 1A). One-way ANOVA demonstrated significant inter-group differences for MTT responses ($p=0.001$). Post hoc tests revealed significantly higher levels of MTT in the FBS-stimulated relative to the other conditions, and reduced MTT in TGF-β relative to EGF- and TGF-α-stimulated cultures (Figure 1D). H33342 fluorescence, reflecting the culture cellular abundance, mainly increased with FBS concentration (Figure 1B). Inter-group comparison of the areas under the curve was significant ($p<0.0001$; Table 1) and notable for progressively higher cell densities in TGF-α, followed by TGF-β, and then FBS relative to EGF (Figure 1E). Although EGF stimulation had subtle effects on H33342 (cell density), the calculated MTT/H33342 ratios were sharply higher than with the other three culture conditions (Figure 1C). One-way ANOVA of the area under the curve data demonstrated significant inter-group differences ($p=0.0002$), and the post hoc test confirmed robust stimulatory effects of EGF on metabolic activity/cell number (MTT/H33342) relative to the other conditions (Figure 1F).

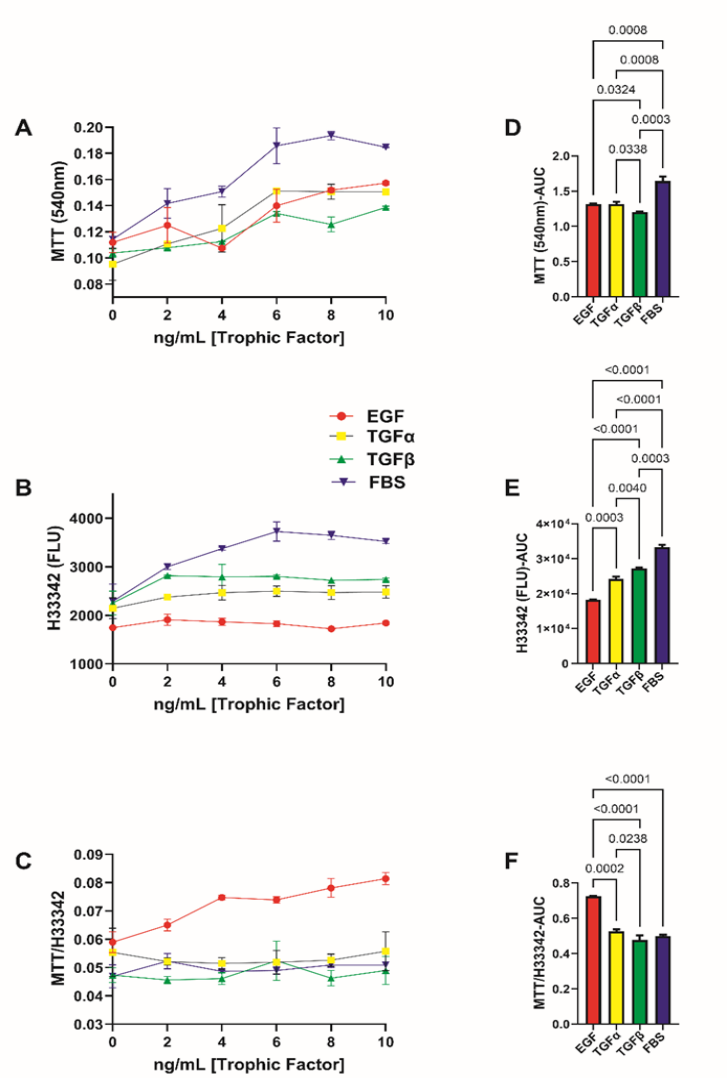

Figure 1: EGF Pathway Stimulation of PNET2 Neuronal Cells: Effects of increasing concentrations (ng/mL) of EGF, TGFα, and TGFβ, and percent FBS (0-10%) on (A) MTT activity, (B) H33342 fluorescence, and (C) MTT activity normalized to culture cell density (MTT/H33342). Graphs corresponding to the area-under-the-curve analysis of dose-dependent growth factor stimulation are shown in Panels (D) MTT, (E) H33342, and (F) MTT/H33342. Results (mean ± S.D.) were obtained from three replicate cultures per data point. Inter-group comparisons were made by one-way ANOVA with post hoc Tukey tests (see Table 1). Significant (p≤0.05) differences are displayed. FLU= fluorescence light units.

EGFR Inhibitor Effects on Neuronal Metabolism and Growth

To confirm the role of EGFR pathway activation for promoting neuronal metabolism and survival/growth, 96-well PNET2 cultures were treated with dose ranges of the EGFR inhibitors, AG1478 and Gefitinib (ZD1839) for 24 hours. AG1478 is a potent EGFR tyrosine kinase inhibitor that has an IC_{50} of 3 nM. Gefitinib (ZD1839) is an EGFR tyrosine kinase phosphorylation inhibitor that has an IC_{50} of 25 to 60 nM. The dose-response curves were analyzed using log-linear regression to determine whether the slopes differed significantly from zero and to compute the coefficient of determination (R2) for the dose-response

relationship (Figure 2). At the lowest concentrations, AG1478 (Figure 2A) and Gefitinib (Figure 2D) had modest effects on MTT activity, but as the doses approached and exceeded the IC_{50}s, MTT activity progressively declined. Both slopes differed significantly from zero; for AG1478, the r^2= 0.5788, and for Gefitinib r^2= 0.3142. H33342 fluorescence remained relatively stable across most of the dose ranges but declined sharply above the AG1478 IC_{50}s (r^2= 0.8706; Figure 2B). In contrast, H33342 fluorescence varied with dose but without a clear trend, accounting for the very low correlation, r^2= 0.068 (Figure 2E). The curves for MTT/H33342 were complex (Figures 2C, 2F). For cells treated with AG1478, overlap of reduced MTT with cell loss resulted in very low MTT/H33342 ratios. The tail-end increase in MTT/H3334 was due to greater cell loss compared with the decline in MTT. The biphasic curve produced an r^2= 0.0452 (Figure 2C). The curves corresponding to Gefitinib's effects on H33342 (Figure 2E) and MTT/H33342 (Figure 2F) were largely similar. These studies primarily demonstrate that EGFR inhibitors markedly inhibit MTT activity, suggesting that EGF pathway stimulation plays a dominant role in supporting neuronal metabolic function, followed by cell viability and growth.

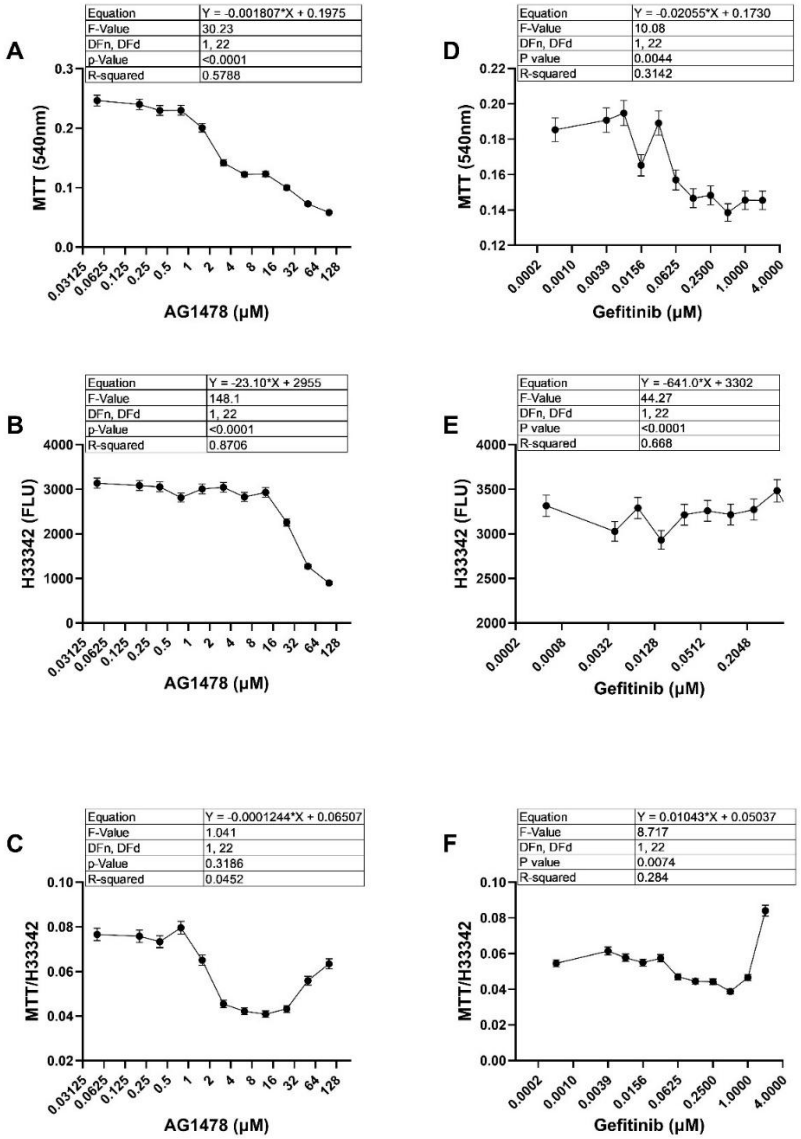

Figure 2: EGFR Inhibitor Effects on MTT Activity and H33342 Fluorescence. PNET2 96-well cultures were treated with increasing concentrations of the (A-C) AG1478 or (D-F)

Gefintib EGFR inhibitor for 24h. Each condition included 8 replicate cultures. Graphs show the mean ± S.D. of (A, D) MTT activity, (B,E) H33342 fluorescence, and (C, F) MTT/H33342. The curves were subjected to log-linear regression analysis to assess whether the slopes differed significantly from zero and to calculate the R-squared (goodness of fit). The results are shown in the tables above each graph. FLU= fluorescence light units.

EGF Pathway Activation

The next goal was to determine the effects of each trophic factor on EGFR signaling and potential downstream targets. ELISAs measured EGFR, tyrosine phosphorylated EGFR (pY-EGFR), proliferating cell nuclear antigen (PCNA), a marker of cell growth, ASPH-A85G6, ASPH-FB50, and RPLPO with results normalized to protein content in the wells. Results from 5 replicate cultures were analyzed by one-way ANOVA (Table 2) and are displayed with boxplots/whiskers (Figure 3).

Table 2: ANOVA Test Results of Trophic Factor-Stimulated PNET2 Cells

Molecule	F-Ratio	p-Value
EGFR	2.22	N.S.
pY-EGFR	6.57	0.0014
PCNA	6.31	0.0017
ASPH-A85G6	4.21	0.0128
ASPH-FB50	2.29	0.097
RPLPO	0.73	N.S.

PNET2 cells were stimulated with vehicle (0.5% FBS) or 10 nM EGF, TGF-α, or TGF-ß. Immunoreactivity was measured by ELISA in 5 replicate cultures. Intergroup comparisons were made by one-way ANOVA with post hoc Tukey tests (See Figure 3).

Post hoc Tukey tests demonstrated significant trophic factor effects on pY-EGFR (Figure 3B), PCNA (Figure 3C), and ASPH-A85G6 (Figure 3D), and a statistical trend effect ($0.05<p<0.10$) was observed for ASPH-FB50 (Table 2; Figure 3E). The levels of pY-EGFR were significantly elevated in EGF, TGF-α, and TGF-ß stimulated cultures relative to vehicle (Figure 3B). PCNA was also significantly elevated in trophic factor-stimulated relative to vehicle, and TGF-α produced the greatest effect (Figure 3C). ASPH-A85G6 immunoreactivity was significantly increased by EGF compared with Vehicle, TGF-α, and TGF-ß (Figure 3D). In contrast, the mean levels of EGFR (Figure 3A), ASPH-FB50 (Figure 3E), and RPLPO (Figure 3F) were similar across the different culture stimulations.

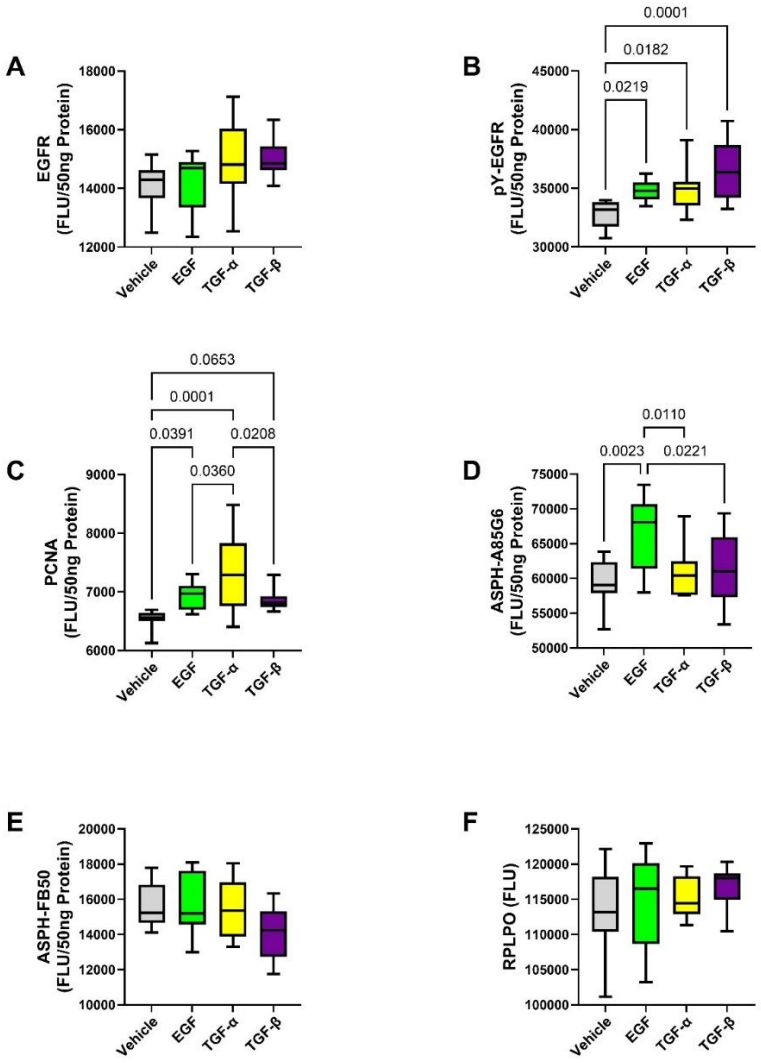

Figure 3: EGF Pathway Activation: Effects of EGF, TGF-α, and TGF-β stimulation of (A) EGFR, (B) tyrosine phosphorylated EGFR (pY-EGFR), (C) proliferating cell nuclear antigen (PCNA), (D) full-length aspartyl-asparaginyl-β-hydroxylase (ASPH-A85G6), and (E) truncated ASPH (ASPH-FB50) expression were compared to Vehicle control (0.5% FBS). (F) RPLPO is a housekeeping control molecule. Immunoreactivity in 5 replicate cultures was measured in replicates of four by ELISA with results normalized to protein content. Inter-group comparisons were made by one-way ANOVA (Table 2) with post hoc Tukey tests. Significant differences ($p \leq 0.05$) are shown within the panels. FLU= fluorescence light units.

EGF Pathway Crosstalk with Insulin/IGF Networks

Neuronal growth, viability, metabolic function, and ASPH expression were shown to be strongly regulated by insulin/IGF-stimulated networks [22, 38, 58]. An important question was whether the stimulatory effects of EGF, TGF-α, and TGF-β on EGFR pathway activation were mediated by crosstalk with insulin/IGF signaling networks. The approach was to utilize custom Quantigene 2 panels to measure mRNA abundance associated with growth factor stimulation (See Methods; Table S4). Two-way ANOVA tests were clustered to compare the

effects of trophic factor stimulation on the expression of growth factors (*INSULIN*, *IGF1*, and *IGF2*), growth factor receptors (*INSULINR, IGF1R*, and *IGF2R*), and insulin receptor substrate molecules (*IRS1, IRS2*, and *IRS4*). Two-way ANOVA tests demonstrated significant effects of trophic factor stimulation (EGF, TGF-α, and TGF-ß) on the expression of growth factors (*INSULIN, IGF1*, and *IGF2*), growth factor receptors (*INSULINR, IGF1R*, and *IGF2R*), and IRS genes (*IRS1*, *IRS2*, and *IRS4*).

Table 3: PNET2 Cells- EGFR Pathway Crosstalk with Insulin/IGF/IRS Network

Genes	Pathway Genes (F-Ratio)	p-value	Trophic Factor Stimulation (F-Ratio)	p-value	Pathway Genes x Trophic Factor Stimulation (F-Ratio)	p-Value
INSULIN, IGF1, IGF2	*2.76*	*0.064*	**497.5**	**<0.0001**	**4.54**	**0.003**
INSULINR, IGF1R, IGF2R	**9.30**	**0.001**	**10.64**	**0.0001**	*2.32*	*0.066*
IRS1, IRS2, IRS4	**3.910**	**0.021**	**525.0**	**<0.0001**	1.51	N.S.

PNET2 cells were stimulated with vehicle (0.5% FBS) or 10 nM EGF, TGF-α, or TGF-ß. Gene expression was measured using a custom Quantigene 2.0 multiplex hybridization panel. Trophic factor genes included *INSULIN, IGF1, and IGF2*. Trophic factor receptor genes included *INSULIN RECEPTOR (INSULINR), IGF1R, and IGF2R*. Insulin receptor substrate (IRS) genes included *IRS1*, *IRS2*, and *IRS4*. Intergroup comparisons were made by two-way ANOVA with post hoc Tukey tests (See Figure 4).

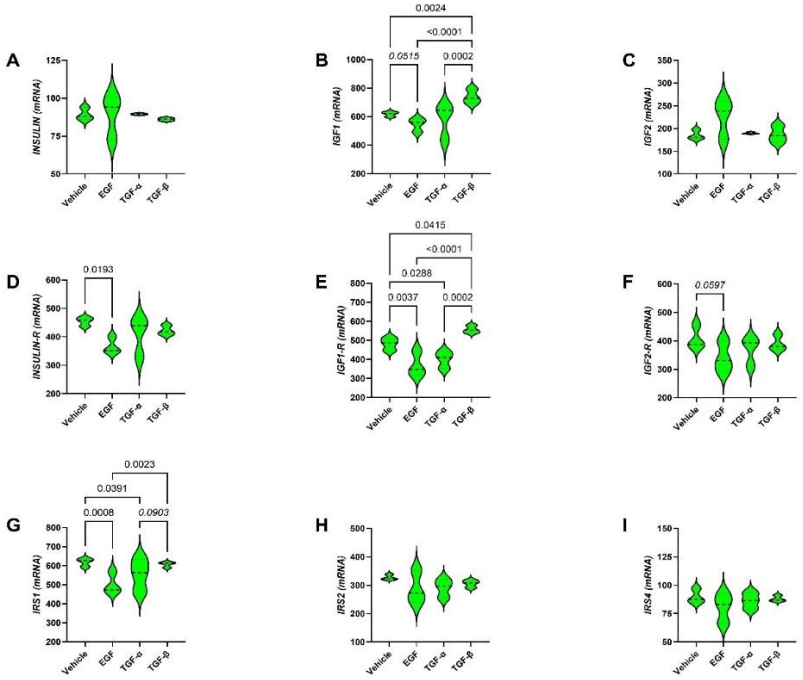

Figure 4: EGF Pathway Crosstalk with upstream components of insulin/IGF signaling networks: Experiments examined the effects of EGF, TGFα, and TGF-ß relative to vehicle (0.5% FBS) on the expression of (A) *INSULIN*, (B) *IGF1*, and (C) *IGF2* growth factors, (D) *INSULINR*, (E) *IGF1R*, (F) *IGF2R*, (G) *IRS1*, (H) *IRS2*, and (I) *IRS4* mRNA transcripts. Gene expression was measured using a multiplex RNA hybridization panel with results normalized to housekeeping genes. Violin plots display the distribution of results from 4 replicate cultures per group. Inter-group comparisons were made by

one-way ANOVA (Table 3) and post hoc Tukey tests. Significant differences (p≤0.05) or statistical trendwise effects (*0.05 < p < 0.10*) are shown within the panels.

In addition, significant effects were observed with respect to the growth factor receptor and IRS genes, and interactions between trophic factors stimulation x the growth factor target genes (*INSULIN, IGF1*, and *IGF2*). A statistical trend effect (0.05 < p <0.10) was also detected for the interaction between growth factor receptor genes x trophic factor stimulation (Table 3). The graphs and post hoc tests demonstrated significant intergroup differences restricted to IGF1, such that TGF-β significantly increased IGF1 mRNA relative to all other treatments, whereas under EGF stimulation, IGF1 was significantly reduced relative to the effects of TGF-β, and trendwise reduced relative to vehicle (Figure 4B). The *INSULIN* (Figure 4A) and *IGF2* (Figure 4C) mRNA levels were not modulated by trophic factor stimulation.

Regarding the insulin/IGF receptors, the major intergroup differences were centered on *IGF1R*, which showed significantly reduced mRNA levels in cultures stimulated with EGF or TGF-α and higher levels in TGF-β-stimulated cultures relative to the other three groups (Figure 4E). In addition, EGF significantly reduced INSULINR (Figure 4D) and trendwise reduced IGF2R (Figure 4F) relative to vehicle. Regarding *IRS* genes, the post hoc Tukey tests demonstrated significant or trendwise reductions in *IRS1* in EGF- and TGF-α-stimulated relative to vehicle or TGF-β (Figure 4G). There were no significant or trendwise intergroup differences observed with respect to *IRS2* (Figure 4H) or *IRS4* (Figure 4I).

EGF Pathway Crosstalk with Notch Networks

Exploring the potential role of crosstalk between EGFR and Notch signaling was based on evidence that Notch networks are activated by ASPH's catalytic domain [40, 59-61], and that ASPH expression and function are modulated by insulin/IGF stimulation [26, 62]. Therefore, it was important to determine if the stimulatory effects of EGFR networks were mediated by crosstalk with Notch pathways. The Notch network mRNA transcripts measured were *NOTCH1, JAGGED1, ASPH, HES1, HEY1, and HIF-1A*. Two-way ANOVA demonstrated significant trophic factor stimulation and Notch pathway receptor/ligand genes, and no interactive effects of receptor/ligand genes x trophic factor stimulation (Table 4). The violin plot) and post hoc Tukey tests revealed similar mRNA levels of *NOTCH1* (Figure 5A), *JAGGED1* (Figure 5B), and *ASPH* (Figure 5C) across the different trophic factor stimulations. In contrast, two-way ANOVA demonstrated significant effects of transcription factor genes, trophic factor stimulation, and their interactive effects (Table 4). The violin plots and post hoc Tukey tests revealed that TGF-β significantly increased HES1 (Figure 5D) and HEY1 (Figure 5E) relative to vehicle, EGF, and TGF-α. In addition, EGF and TGF-α stimulations resulted in lower *HES1* mRNA relative to vehicle (Figure 5D). *HIF1A* was significantly lower in EGF- and TGF-α-stimulated relative to vehicle-treated cultures, and in EGF relative to TGF-β (Figure 5F). In contrast, *HIF1A* was not significantly modulated by TGF-β relative to vehicle.

Table 4: PNET2 Cells- EGFR Pathway Crosstalk with Notch Network

Notch Network	Gene Factor (F-Ratio)	p-value	Trophic Factor (F-Ratio)	p-value	Gene x Trophic Factor (F-Ratio)	p-Value
Receptors/Ligands	**1182**	**<0.0001**	1.691	N.S.	1.168	N.S.
Transcription Factors	**644.9**	**<0.0001**	**29.87**	**<0.0001**	**16.39**	**<0.0001**
Control Genes	**3197**	**<0.0001**	0.456	N.S.	1.618	N.S.

PNET2 cells were stimulated with vehicle (0.5% FBS) or 10 nM EGF, TGF-α, or TGF-β. Gene expression was measured using a custom Quantigene 2.0 multiplex hybridization panel. Receptor/Ligand-related genes included *NOTCH1, JAGGED1*, and *ASPH*. Transcription factor-related genes included *HES1*, *HEY1*, and *HIF-1a*. Control Genes included *ABCG2*, *CASR*, *HPRT1*, AND *RPL13a*. Intergroup comparisons were made by two-way ANOVA with post hoc Tukey tests (See Figures 5 and 7).

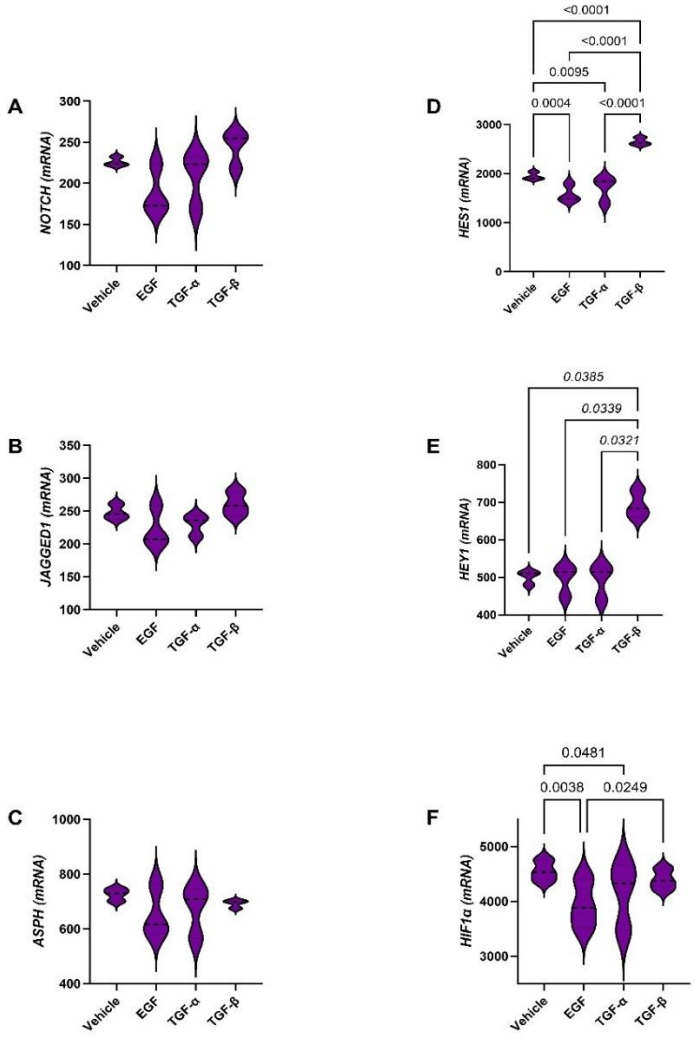

Figure 5: EGF Pathway Crosstalk with Notch Networks: These studies examined the effects of EGF, TGFα, and TGF-β relative to vehicle on the expression of (A) *NOTCH1*, (B) *JAGGED1*, (C) *ASPH*, (D) *HES1*, (E) *HEY1*, and (F) *HIF-1a* mRNA transcripts. Gene expression was measured using a multiplex RNA hybridization panel with results normalized to housekeeping genes. Violin plots display the distribution of results from 4 replicate cultures per group. Inter-group comparisons were made by one-way ANOVA (Table 4) and post hoc Tukey tests. Significant differences (p≤0.05) and statistical trendwise effects (*0.05 < p < 0.10*) are shown within the panels.

Additional studies examined the effects of the ZLDI-8 and GI254023X Notch inhibitors on MTT activity (Figures 6A, 6D), H33342 fluorescence (Figures 6B, 6E), and the relative levels of MTT/H33342 (Figures 6C, 6F) to assess the role of Notch pathway activation on CNS neuronal metabolic activity and viability. With increasing concentration of either Notch inhibitor, MTT activity declined progressively. In contrast, H33342 fluorescence remained stably high (like Vehicle-treatment) except for sharp declines that occurred close to or beyond the IC_{50}s of ZLDI-8 (31.6 μM) and GI254023X (5.3 nM). The curves for MTT/H33342 were complex but largely mirrored MTT, except for increases at the highest doses of either inhibitor, likely reflecting stress responses.

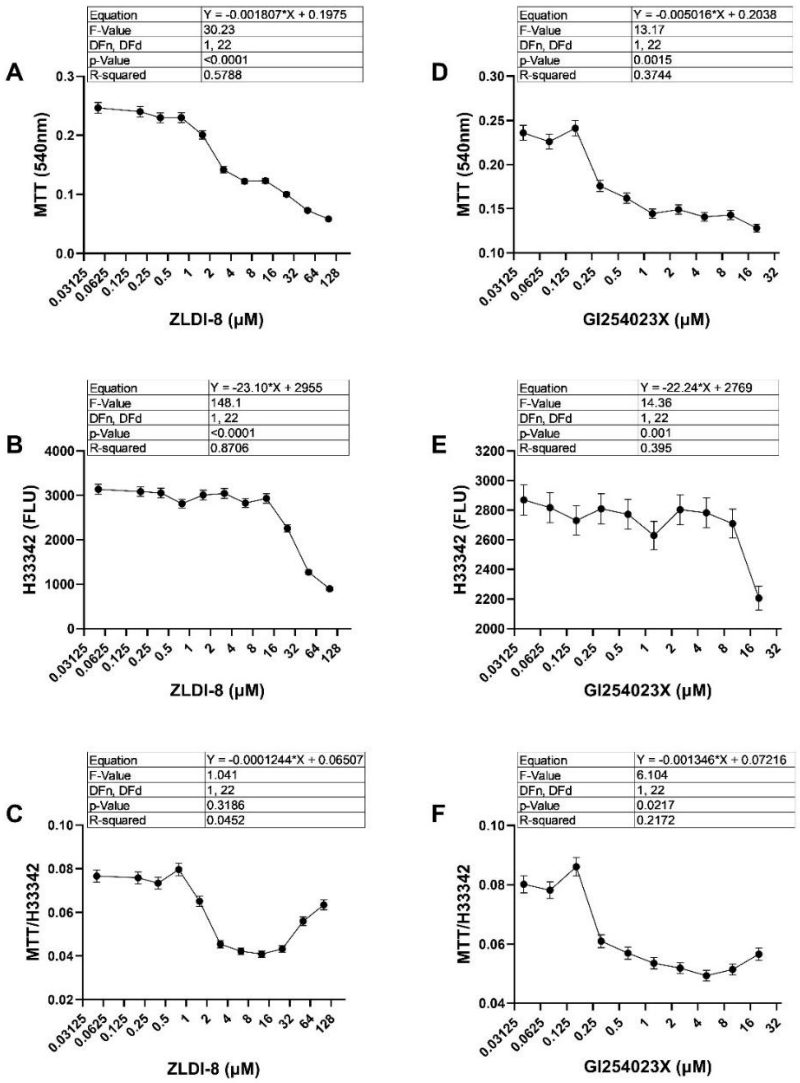

Figure 6: Notch Inhibitor Effects on MTT Activity and H33342 Fluorescence. PNET2 96-well cultures were treated with increasing concentrations of the (A-C) ZLDI-8 or (D-F) G1254023X Notch inhibitor for 24h. Each condition included 8 replicate cultures. Graphs show the mean ± S.D. of (A, D) MTT activity, (B, E) H33342 fluorescence, and (C, F) MTT/H33342. The curves were subjected to log-linear regression analysis to assess whether the slopes differed significantly from zero and to calculate the R-squared (goodness of fit). The results are shown in the tables above each graph.

Control Gene Studies

The Quantigene 2.0 assays included simultaneous analysis of control genes (*ABCG2*, *CASR*, *HPRT1*, and *RPL13a*). Two-way ANOVA detected significant variances in the expression of different control genes, but no significant trophic factor stimulation or trophic factor x control mRNA interactive effects (Table 4). The corresponding graphs showed similar levels of ABCG2 (Figure 7A), CASR (Figure 7B), HPRT1 (Figure 7C), and RPL13a (Figure 7D) mRNA across the different trophic factor stimulations.

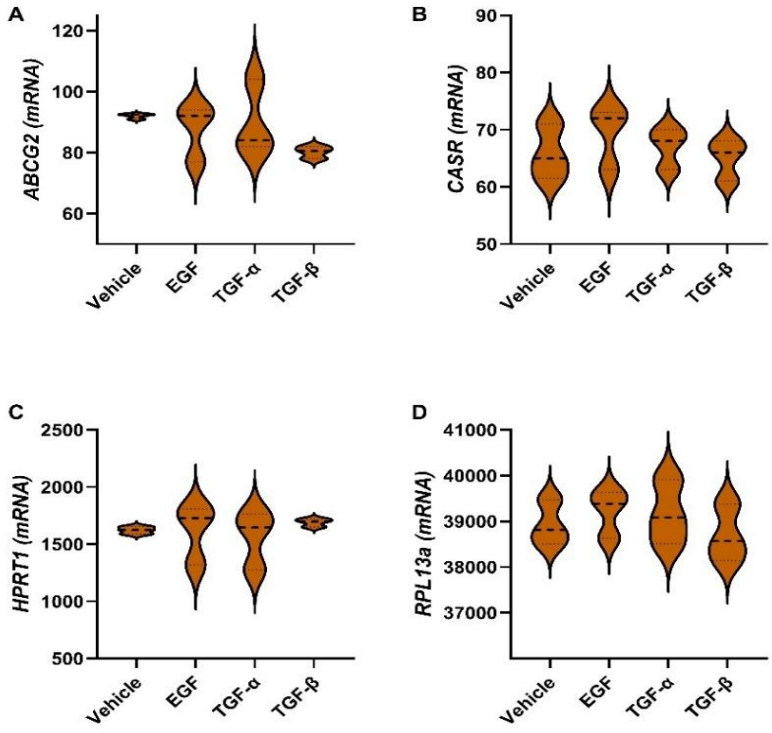

Figure 7: Trophic Factor Stimulation Does Not Modulate Expression of Control Genes. The effects of EGF, TGF-α, and TGF-ß on the expression of (A) *ABCG2*, (B) *CASR*, (C) *HPRT1*, and (D) *RPL13a* relative to vehicle were examined using a multiplex RNA hybridization panel. Violin plots display the distributions of results from 4 replicate cultures per group. Inter-group comparisons were made by one-way ANOVA (Table 4) and post hoc Tukey tests.

Ethanol Effects on EGFR and Erk-MAPK Signaling

The second phase of this research investigated ethanol's effects on EGF-related trophic factor stimulation of PNET2 neuronal cells. The goal was to assess how ethanol exposure impacts EGFR signaling and responses to EGF pathway trophic factor stimulation. Control and ethanol-exposed PNET2 cells, stimulated for 48h with vehicle (0.5% FBS), EGF, TGF-α, or TGF-ß, were used to measure EGFR, pY-EGFR, PCNA, ASPH-A85G6, and ASPH-FB50 by ELISA. Two-way ANOVA tests detected significant ethanol effects on pY-EGFR, PCNA, and ASPH-A85G6, significant trophic factor stimulation effects on EGFR, pY-EGFR, PCNA, and A85G6, and significant ethanol x trophic factor stimulation interactive effects for pY-EGFR and ASPH-A85G6 (Table 5).

Table 5: PNET2 Cells: Ethanol Effects on Trophic Factor Stimulation Effects on EGFR Pathway Molecules

	Ethanol Effect (F-Ratio)	p-value	Trophic Factor Effect (F-Ratio)	p-value	Ethanol x Trophic Factor (F-Ratio)	p-Value
EGFR	3.77	*0.061*	**4.423**	**0.010**	0.430	N.S.
pY-EGFR	**18.02**	**0.0002**	**24.33**	**<0.0001**	**4.056**	**0.015**
PCNA	**7.29**	**0.011**	**6.66**	**0.0013**	0.916	N.S.
ASPH-A85G6	**58.42**	**<0.0001**	**46.90**	**<0.0001**	**3.009**	**0.045**
ASPH-FB50	1.43	N.S.	0.29	N.S.	1.37	N.S.

Control and ethanol-exposed PNET2 cells were stimulated with trophic factors (Vehicle, EGF, TGF-α, or TGF-β) for 24 hours. Protein homogenates were used to measure immunoreactivity by ELISA, with results normalized to protein content. Two-way ANOVA test results examining the effects of ethanol exposure, trophic factor stimulation, and ethanol x trophic factor interactions. Each group and condition included 5 replicate cultures. See Figure 8 for post hoc Tukey test results.

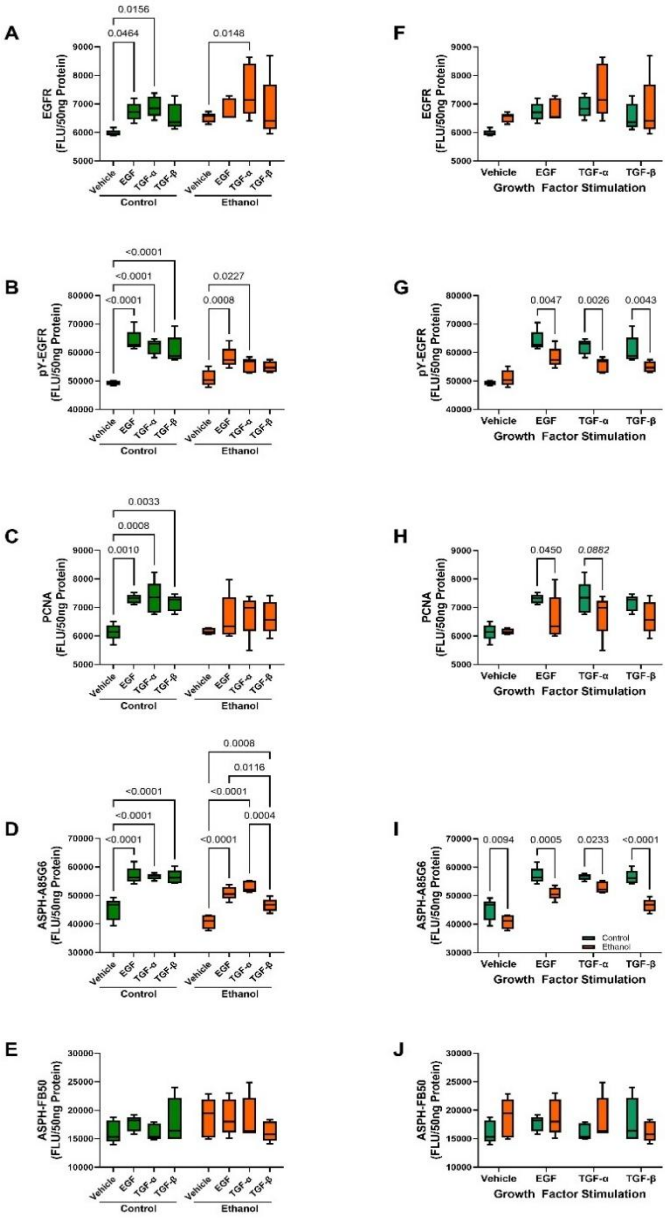

Figure 8: Ethanol Effects on EGF Pathway Activation and Function: Control and ethanol-exposed PNET2 cultures (n=5/treatment/group) were stimulated with vehicle

(0.5% FBS) or 10nM EGF, TGF-α, or TGF-β for 24h. Immunoreactivity to (A, F) EGFR, (B, G) tyrosine phosphorylated EGFR (pY-EGFR), (C, H) proliferating cell nuclear antigen (PCNA), (D, I) ASPH-A85G6, and (E, J) ASPH-FB50 was measured by ELISA, and results were normalized to protein concentration. Inter-group comparisons were made by two-way ANOVA (Table 5) and post hoc Tukey tests. The results are graphed to depict the significant (A-E) within-group (control or ethanol) and (F-J) between-group (control versus ethanol) differences. Significant differences ($p \leq 0.05$) and statistical trendwise effects ($0.05 < p < 0.10$) are shown within the panels. FLU= fluorescence light units.

The graphed results are plotted to illustrate both the within-group effects of trophic factor stimulation (Figures 8A-8E) and between-group, i.e., control versus ethanol effects on EGFR, pY-EGFR, PCNA, ASPH-A85G6, and ASPH-FB50 (Figure 8F-8J). In control cultures, EGF, TGF-α, and TGF-β significantly increased pY-EGFR (Figure 8B), PCNA (Figure 8C), and ASPH-A85G6 (Figure 8D), whereas only EGF and TGF-α increased EGFR relative to vehicle (Figure 8A). In ethanol-treated cultures, only TGF-α stimulated EGFR; both EGF and TGF-α stimulated pY-EGFR; and EGF, TGF-α, and TGF-β each stimulated ASPH-A85G6 (Figure 8D).

ASPH-FB50 was not significantly modulated by trophic factor stimulation in either the control or ethanol-treated PNET2 cultures (Figure 8E). Post hoc Tukey tests to assess the relative effects of ethanol on trophic factor-stimulated protein expression revealed significant reductions in EGF-, TGF-α-, and TGF-β-stimulated pY-EGFR (Figure 8G) and ASPH-A85G6 (Figure 8I). In addition, ethanol significantly reduced EGF- and TGF-α-stimulated PCNA (Figure 8H). In contrast, there were no significant effects of ethanol on trophic factor-stimulated levels of EGFR (Figure 8F) or ASPH-FB50 (Figure 8J).

Growth factor and ethanol effects on p44/42 MAPK (Erk1/2) and phosphotyrosine (pY)-p44/42 MAPK (Erk1/2) were assessed by ELISA. In addition, the calculated ratios of pY-p44/42 MAPK (Erk1/2) /Total p44/42 MAPK (Erk1/2), reflecting relative levels of phosphorylation, were compared. Two-way ANOVA tests demonstrated significant ethanol effects on p44/42 MAPK (Erk1/2) and pY/T-p44/42 MAPK (Erk1/2), and significant growth factor effects on p44/42 MAPK (Erk1/2), pY-p44/42 MAPK (Erk1/2), and pY/T-p44/42 MAPK (Erk1/2) (Table 6). In addition, significant ethanol x trophic factor interactive effects were observed with respect to pY-p44/42 MAPK (Erk1/2) and pY/T-p44/42 MAPK (Erk1/2). In the control group, the post hoc Tukey tests demonstrated that EGF and TGF-α but not TGF-β signaling through pY-EGFR significantly increased p44/42 MAPK (Erk1/2)(Figure 9A), and only TGF-α stimulated pY-p44/42 MAPK (Erk1/2). The relative reduction in pY/T-p44/42 MAPK (Erk1/2) observed in the EGF-stimulated cultures resulted from elevated expression of p44/42 MAPK (Erk1/2) without a corresponding increase in tyrosine phosphorylation (Figure 9C). In the ethanol-exposed cultures, TGF-α increased p44/42 MAPK (Erk1/2), mirroring the control group's response (Figure 9A). However, the ethanol-exposed, vehicle-treated cultures had the highest levels of pY-p44/42 MAPK (Erk1/2) (Figure 9C) and pY/T-p44/42 MAPK (Erk1/2)(Figure 9E), indicating that EGF, TGF-α, and TGF-β trophic factor stimulation had suppressive effects relative to vehicle. Post hoc tests to detect ethanol-mediated effects revealed significantly higher levels of pY-P44/42 MAPK (Figure 9D) and pY/T-p44/42 MAPK (Erk1/2) (Figure 9F) in the vehicle+ethanol-treated relative to corresponding control cultures. In addition, the levels of pY/T-p44/42 MAPK (Erk1/2) (Figure 9F) were significantly

higher in ethanol-treated versus control EGF- and TGF-ß-stimulated cultures. The main inhibitory effects of ethanol were due to reduced EGF- and TGF-ß-stimulated p44/42 MAPK (Erk1/2)immunoreactivity (Figure 9B).

Table 6: PNET2 Cells: Ethanol Effects on Trophic Factor Stimulation of p44/42 MAPK (Erk1/2)

	Ethanol Effect (F-Ratio)	p-value	Trophic Factor Effect (F-Ratio)	p-value	Ethanol x Trophic Factor (F-Ratio)	p-Value
p44/42 MAPK (Erk1/2)	**7.885**	**0.0066**	**8.003**	**0.0001**	1.249	N.S.
pY-p44/42 MAPK (Erk1/2)	1.64	N.S.	**5.837**	**0.0014**	**3.651**	**0.017**
pY/T-p44/42 MAPK (Erk1/2)	**28.74**	**<0.0001**	**22.87**	**<0.0001**	**6.478**	**0.0007**

Control and ethanol-exposed PNET2 were stimulated with trophic factors (Vehicle, EGF, TGF-α, or TGF-ß) for 24 hours. Protein homogenates were used to measure immunoreactivity by ELISA with results normalized to protein content. Two-way ANOVA test results show the effects of ethanol exposure, trophic factor stimulation, and ethanol x trophic factor interactions. Each group and condition included 10 replicate cultures. See Figure 9 for post hoc Tukey test results.

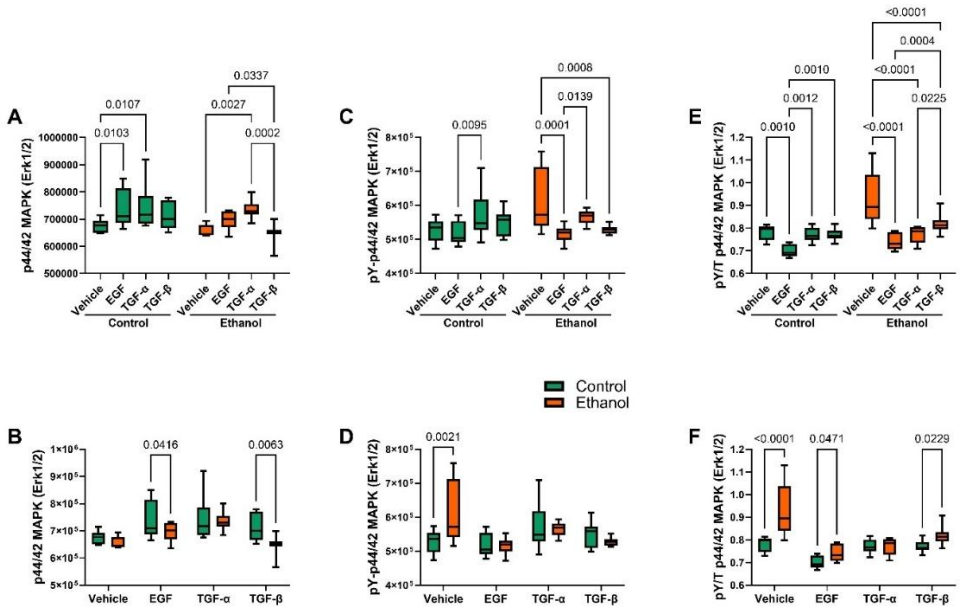

Figure 9: Trophic Factor Effects on p44/42 MAPK (Erk1/2) Signaling: Control and ethanol-exposed PNET2 neuronal cultures (n=10/treatment/group) were stimulated with vehicle (0.5% FBS) or 10nM EGF, TGF-α, or TGF-ß for 24h. Box-and-whiskers plots depict the median and range of immunoreactivity to (A, B) p44/42 MAPK (Erk1/2) and (C, D) pY-p44/42 MAPK (Erk1/2) measured by duplex ELISA with results normalized to protein concentration. (E, F) The calculated ratios of pY-p44/42 MAPK (Erk1/2) to total (T) p44/42 MAPK (Erk1/2) reflect relative levels of phosphorylation. Inter-group comparisons were made by two-way ANOVA (Table 6) and post hoc Tukey tests. The results are graphed to display the significant (A, C, E) within-group (control or ethanol) or (B, D, F) between-group (control versus ethanol) differences. Significant differences (p≤0.05) are shown within the panels.

Ethanol's Cytomorphologic Effects on EGF Pathway Stimulation

The morphological changes associated with trophic factor stimulation and ethanol exposure were documented with Crystal Violet-stained cytospin preparations of the cultured PNET2 cells (Figure 10). Vehicle-treated control cells exhibited prominent nucleoli, coarse surface membrane blebbing, and apparent cell fusion, possibly reflecting incomplete mitosis (Figure 10A).

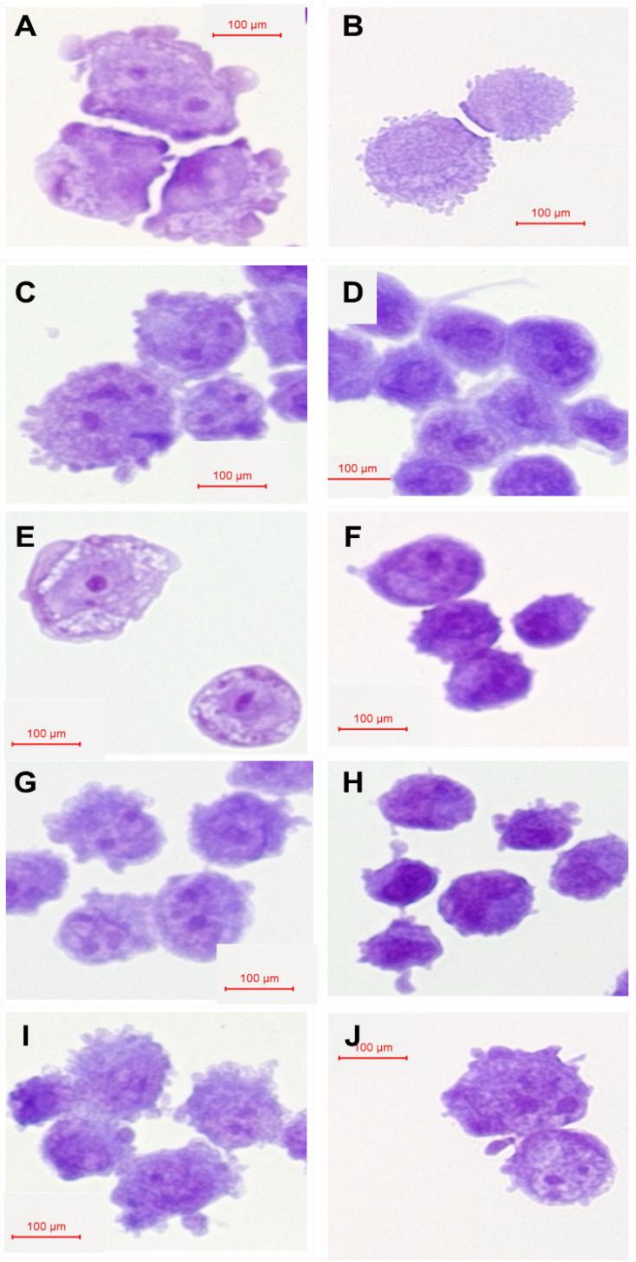

Figure 10: Trophic Factor and Ethanol Effects on PNET2 Neuronal Morphology: (A, C, E, G, I) Control and (B, D, F, H, J) ethanol-exposed PNET2 cells were stimulated with (A, B) Vehicle, (C, D) insulin, (E, F) IGF1, (G, H) EGF, or (I, J) TGF-ß for 48 hours. Cytospin preparations were stained with Crystal violet, examined by light microscopy, and photographed at 400x. Cropped images are used to illustrate cellular morphology. Scale bars are included in the panels. Fine arrows =prominent nucleoli; triangles = surface membrane blebs; arrowheads = vacuolation of cytoplasm; circles = nuclear condensation and hyperchromicity.

The ethanol-treated, vehicle-stimulated cultures exhibited a marked reduction in nuclear and nucleolar detail, no mitotic activity, and abundant fine surface-membrane stippling (Figure 10B). The effects of insulin and IGF-1 stimulation were included for comparison due to their known support of PNET2 cell growth and survival [22, 26, 63]. Insulin- (Figure 10C) and IGF-1- (Figure 10E) stimulated control cells exhibited prominent nucleoli. In addition, the insulin-stimulated cells exhibited finer circumferential membrane surface blebbing relative to vehicle, while the IGF-1-stimulated cells had smooth surfaces and conspicuous cytoplasmic/perinuclear vacuolation (Figure 10E). Ethanol-treated insulin- (Figure 10D) or IGF-1-stimulated (Figure 10F) cultures had conspicuously smaller cells with dense nuclear staining, indistinct nucleoli, and minimal surface membrane processes. EGF (Figures 10G, 10H) and TGF-ß (Figures 10I, 10J) stimulation increased the number of short surface membrane processes in control (Figures 10G, 10I) and ethanol-exposed (Figure 10H, 10J) cells, however, nucleolar delineation was evident only in control cultures, possibly due to nuclear hyperchromasia and condensation in the ethanol-treated cultures. TGF-ß was the only trophic factor that enhanced nucleolar detail, caused cellular enlargement, and enhanced the appearance of surface processes in ethanol-exposed cultures. Importantly, the cytomorphology of TGF-ß-treated ethanol-exposed cells (Figure 10J) most closely resembled control cells treated with TGF-ß, EGF, or insulin.

Ethanol Effects on Cerebellar EGF Pathway Activation

The third phase of this study was to validate the in vitro results using cerebellar tissue from an in vivo/ex vivo FASD model generated in Long Evans rat pups. The cerebellum is one of the important CNS targets of alcohol-related brain damage across the lifespan. The goal was to assess how developmental exposures to ethanol impact EGFR signaling and responses to EGFR pathway trophic factor stimulation in the brain.

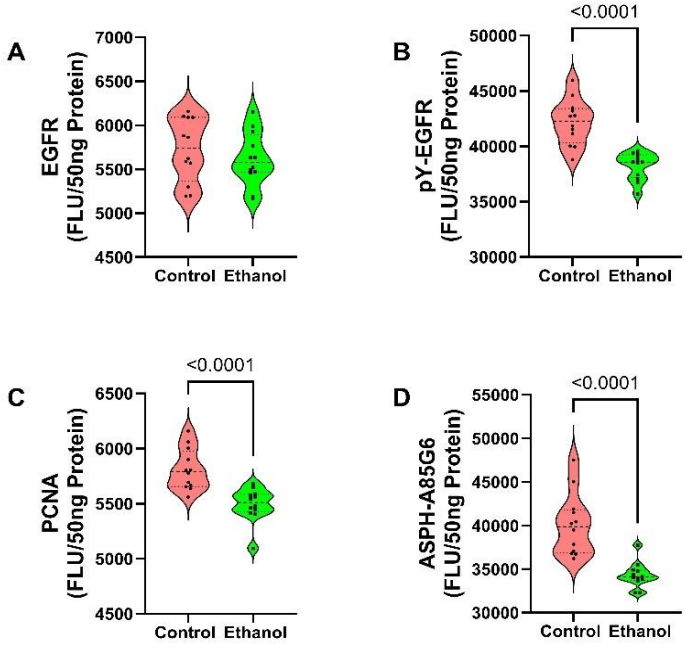

Figure 11: Validation Studies Using an In Vivo FASD Model: A rat FASD model generated by developmental binge ethanol administration was used to examine the in vivo effects on (A) EGFR, (B) pY-EGFR, (C) PCNA, and (D) ASPH expression in cerebellar

tissue. Immunoreactivity was measured by ELISA, and results were normalized to protein content. Violin plots display the distribution of results from 12 replicate samples per group. Inter-group comparisons were made with Welsh t-tests. Significant differences (p≤0.05) are shown within the panels. FLU= fluorescence light units.

The model was generated by intraperitoneal binge administration of ethanol to rat pups. Cerebellar immunoreactivity to EGFR, pY-EGFR, PCNA, and ASPH-A85G6 was measured by duplex ELISA, and the intergroup statistical comparisons were made using the Welch T-test. Control and ethanol-exposed cerebellar tissue had similar levels of EGFR immunoreactivity (Figure 11A), whereas ethanol significantly reduced the mean levels of pY-EGFR (Figure 11B), PCNA (Figure 11C), and ASPH-A85G6 (Figure 11D).

Ethanol Effects on Trophic Factor Stimulation of EGF Pathways in Cerebellar Tissue

Cerebellar slice cultures generated from binge ethanol-exposed and vehicle-treated rat pups were stimulated with vehicle, or 20 nM EGF, TGF-α, or TGF-β for 24h. The slices were harvested to extract proteins for duplex ELISA measurements of EGFR, pY-EGFR, PCNA, ASPH-A85G6, and ASPH-FB50. Two-way ANOVA demonstrated significant ethanol effects on pY-EGFR, PCNA, and ASPH-A85G6, and a statistical trend effect on EGFR (Table 7). Significant trophic factor stimulation effects were observed for all molecules except ASPH-FB50. Significant or trendwise ethanol x trophic factor interactive effects were observed for pY-EGFR, PCNA (trendwise), and ASPH-A85G6.

Table 7: Cerebellar Slice Cultures: Ethanol Effects on Trophic Factor Stimulation Effects on EGFR Pathway Molecules

	Ethanol Effect	p-value	Trophic Factor Effect	p-value	Ethanol x Trophic Factor	p-Value
EGFR	*3.77*	*0.061*	**4.423**	**0.010**	0.430	N.S.
pY-EGFR	**52.30**	**<0.0001**	**26.03**	**<0.0001**	**10.54**	**<0.0001**
PCNA	**39.05**	**<0.0001**	**8.368**	**<0.0001**	*2.498*	*0.077*
ASPH-A85G6	**184.1**	**<0.0001**	**43.06**	**<0.0001**	**5.026**	**0.0057**
ASPH-FB50	1.429	N.S.	0.287	N.S.	1.372	N.S.

Control and ethanol-exposed cerebellar slice cultures were stimulated with trophic factors (Vehicle, EGF, TGF-α, or TGF-β) for 24 hours. Protein homogenates were used to measure immunoreactivity by ELISA, with results normalized to protein content. Two-way ANOVA test results show the effects of ethanol exposure, trophic factor stimulation, and ethanol x trophic factor interactions. Each group and condition included 5 replicate cultures. See Figure 12 for post hoc Tukey test results.

The graphed results are plotted to illustrate within-group effects of trophic factor stimulation (Figures 12A-12E) and between-group, i.e. control versus ethanol effects on EGFR, pY-EGFR, PCNA, ASPH-A85G6, and ASPH-FB50 (Figure 12F-12J). In control cultures, EGF and TGF-α significantly increased EGFR (Figure 12A), and EGF, TGF-α, and TGF-β significantly increased pY-EGFR (Figure 12B), PCNA (Figure 12C), and ASPH-A85G6 (Figure 12D) relative to vehicle. In ethanol-treated cultures, TGF-α stimulated EGFR (Figure 12A), EGF trendwise and TGF-α significantly increased pY-EGFR (Figure 12B), and EGF, TGF-α, and TGF-β stimulated ASPH-A85G6 (Figure 12D).

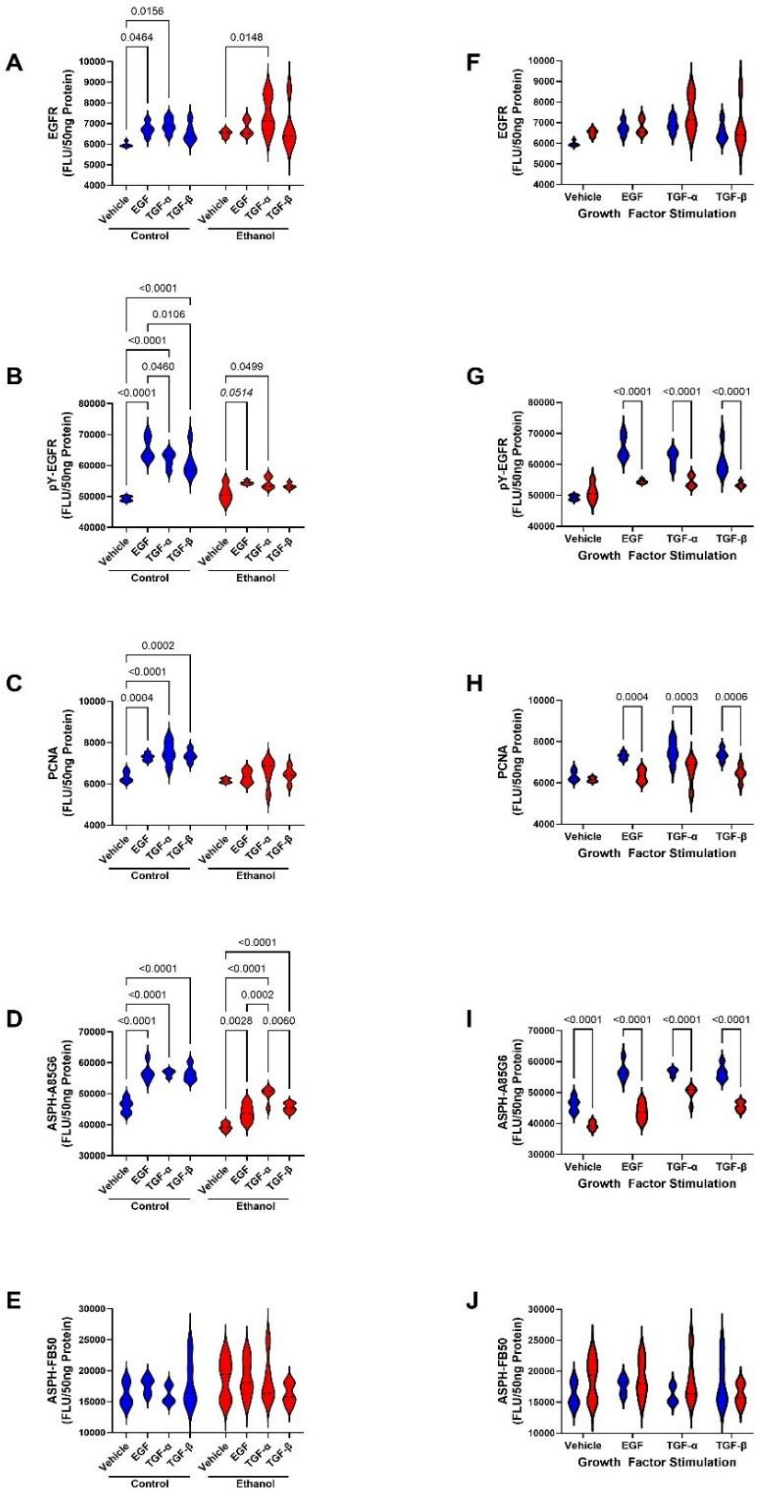

Figure 12: Ethanol Effects on EGF Pathway Activation and Function in Cerebellar Tissue: Control and ethanol-exposed cerebellar slice cultures (n=8/treatment/group) were stimulated with vehicle (0.5% FBS) or 20nM EGF, TGF-α, or TGF-β for 24h. Immunoreactivity to (A, F) EGFR, (B, G) tyrosine phosphorylated EGFR (pY-EGFR), (C, H) proliferating cell nuclear antigen (PCNA), (D, I) ASPH-A85G6, and (E, J) ASPH-FB50 was measured by ELISA, and results were normalized to protein concentration. Inter-group comparisons were made by two-way ANOVA (Table 7) and post hoc Tukey tests. The results are graphed to depict the significant (A-E) within-group (control or

ethanol) or (F-J) between-group (control versus ethanol) differences. Significant differences (p≤0.05) and statistical trendwise effects (*0.05 < p < 0.10*) are shown within the panels. FLU= fluorescence light units.

In addition, TGF-α stimulation produced the highest levels of ASPH-A85G6 in ethanol-exposed cerebella. ASPH-FB50 was not significantly modulated by trophic factor stimulation in either the control or ethanol-exposed cerebellar cultures (Figure 12E). Direct comparisons between the control and ethanol-exposed samples revealed broad, significant inhibitory effects of ethanol on EGF- TGF-α, and TGF-ß stimulated pY-EGFR (Figure 12G), PCNA (Figure 12H), and ASPH-A85G6 (Figure 12I). In addition, unstimulated (vehicle-treated ethanol-exposed cerebellar samples had significantly lower levels of ASPH-A85G6 relative to control (Figure 12I). In contrast, there were no significant ethanol effects on trophic factor-stimulated EGFR (Figure 12F) or ASPH-FB50 (Figure 12J).

DISCUSSION

Previous reports have documented the importance of insulin and IGF signaling networks for supporting growth, survival, migration, plasticity, and metabolism in immature CNS neurons, including cerebellar neurons [22, 23]. In addition, developmental ethanol exposures were shown to have profound inhibitory effects on neuronal growth, survival, migration, and plasticity, linking cerebellar hypoplasia and impaired neuronal migration in fetal alcohol spectrum disorder (FASD) to deficits in insulin and IGF signaling networks and contributing to motor impairments [8-11]. ASPH was identified as a downstream target of insulin/IGF stimulation, regulated at both mRNA and protein levels [26-30]. ASPH has an important role in neurodevelopment because it activates Notch signaling networks [31, 35, 36, 38, 39] which mediate neuronal migration [64-67]. Notch pathway activation has diverse roles, including cell motility, plasticity, and growth [64-67]. Correspondingly, ethanol inhibition of insulin/IGF signaling and ASPH expression during development correlates with FASD-associated impairments in cerebellar neuronal migration [28, 35, 68] and long-term deficits in motor function [2, 7, 69, 70]. However, the finding that these adverse effects of ethanol on ASPH expression and cerebellar structure and function were only partially prevented by treatment with anti-oxidant and insulin-sensitizing agents such as PPAR agonists or dietary soy [68, 71], led to the hypothesis that additional signaling pathways contributed to CNS pathology in FASD.

Interest in EGFR networks stemmed from the realization that EGFR is expressed in the immature brain, including in the cerebellum, yet little is known about the pathway in relation to trophic factor stimulatory effects and sensitivity to prenatal ethanol exposure. EGF signaling has been characterized mainly in non-CNS cells, particularly by malignant neoplasms [72]. Importantly, EGFR signaling is mediated through Erk-MAPK, PI3K-Akt, JAK-STAT, PKC-PLCγ1, and mTOR [72, 73]. However, EGFR signaling can also regulate Notch by inhibiting Notch gene expression and affecting cellular differentiation (74), and Notch1 can regulate EGFR, increasing EGFR mRNA and protein expression [74]. In addition, EGFR signaling can crosstalk with the Wnt pathway (76) through activation, suppression, or transactivation during development and carcinogenesis [75, 76]. Therefore, EGFR and insulin/IGF signaling networks crosstalk and converge on many of the same pathways, suggesting that they also interact. The present study characterized the effects of different

EGFR-responsive trophic factors on PNET2 cell growth, viability, and ASPH expression, and examined the effects of ethanol exposure. Mechanistic experiments examined the direct and indirect effects of EGFR to determine whether these effects were mediated by crosstalk with the insulin/IGF or Notch networks. In addition, experiments were conducted to characterize the effects of ethanol on EGFR signaling in PNET2 cells and to validate these findings in cerebellar tissue from an established experimental model of FASD.

Corresponding with the known expression of EGFR and related signaling networks in the developing cerebellum [47], these studies confirmed EGFR expression and trophic factor tyrosine phosphorylation of EGFR in PNET2 cells, which were derived from a human neuroblastic cerebellar tumor. Although growth and viability were supported by the three trophic factors that either bind and activate EGFR (EGF, TGF-α) or transactivate EGFR (TGF-ß) signaling, the most prominent effects were produced with TGF-β and EGF. Because previous studies have largely focused on the roles of insulin and IGF networks and have provided little information on the contributions of EGFR signaling to cerebellar neuronal growth and viability, these observations are novel and illustrate a broader range of trophic factor regulation in immature cerebellar neurons. The differential effects of EGF, TGF-α, and TGF-ß suggest that the various EGFR-binding/related trophic factors have overlapping but distinct functions in CNS neurons. The critical role of EGFR signaling in neuronal growth and viability was demonstrated using EGFR inhibitors, which caused dose-dependent reductions in cell viability and metabolism.

The studies herein demonstrated for the first time that ASPH is regulated by EGFR signaling activated with EGF, TGF-α, or TGF-ß. Previous studies characterized insulin/IGF-stimulated ASPH expression in various cell types [34, 36, 41, 77, 78] and demonstrated stimulatory effects at both mRNA and protein levels [36]. Overexpression of IRS1, which signals downstream through PI3K-Akt as well as Erk MAPK, increases ASPH expression, although at the protein level, activation of the PI3K-Akt pathway was found to be critical due to inhibition of GSK-3β [39, 40]. However, in addition to full-length ASPH, which contains a C-terminal catalytic domain responsible for hydroxylating and activating Notch [59], insulin and IGF stimulate the truncated homolog, Humbug, which is detectable with the FB50 antibody [31, 77, 78]. Full-length ASPH is detected with the A85G6 antibody, which binds to the C-terminal region of the molecule, which is not expressed in Humbug [48]. Notably, EGFR signaling did not stimulate ASPH-FB50, suggesting divergence in the mechanisms regulating ASPH and Humbug expression, a phenomenon not previously described.

Studies were conducted to determine whether EGFR pathway activation led to crosstalk with the insulin/IGF/IRS or Notch pathways. The results suggest that only TGF-ß results in crosstalk leading to IGF1/IGF1R stimulation, whereas crosstalk via EGF and TGF-α mainly inhibited these pathways. Furthermore, downstream effects of EGFR networks on insulin/IGF signaling were largely inhibitory. In essence, only very proximal steps in the insulin/IGF-Akt pathway, i.e. the IGF-1 and IGF-1R were significantly increased by TGF-ß stimulation. Otherwise, EGF pathway-related trophic factors had inhibitory crosstalk effects on *INSULINR, IGF1R, IGF2R* and/or *IRS1*.

The finding that treatment with Notch inhibitors also reduced growth factor-stimulated PNET2 cell metabolism and viability supports the notion that EGFR signaling cross-talks with Notch and is, in part, regulated by Notch. In contrast to insulin/IGF

networks, analysis of Notch signaling mediators revealed that TGF-ß strongly stimulates two major Notch pathway transcription factors, HES1 and HEY1. Although ASPH mRNA was not significantly increased, its protein (immunoreactivity) was sharply higher in TGF-ß-stimulated cultures. Notch transcription factors were upregulated by TGF-ß but not EGF or TGF-α. Therefore, the most likely mechanism by which EGFR signaling increases ASPH expression via EGF, TGF-α, and TGF-ß is through alternate downstream pathways.

ASPH protein has been shown to be increased by insulin and IGF1 [62], plays a critical role in neuronal migration [35], and functions as a potent activator of Notch [59]. Mechanistically, ASPH, as detected with the A85G6 monoclonal antibody, harbors a catalytic domain critical for Notch hydroxylation, releasing its intracellular domain for nuclear translocation and activation of HES/HEY transcription factors [36, 39, 48]. Therefore, IGF 1 stimulation via TGF-ß increases ASPH protein, which then activates Notch networks. ASPH protein expression increases with insulin/IGF stimulation due to reduced proteolytic degradation [28]. We hypothesize that EGFR activation of ASPH is mediated through mTOR or possibly stress pathways. Previous studies demonstrated that both mTOR and stress linked to HIF-1α can increase ASPH expression and cell motility [38]. Additional studies are needed to further dissect these mechanisms.

The FASD-related experiments were inspired by the finding that interventions designed to restore ethanol-mediated impairments in insulin/IGF signaling, including those linked to inhibition of cerebellar ASPH expression and neuronal migration in FASD, were only partially effective [71]. Little was known about the effects of prenatal alcohol exposure on EGFR signaling in relation to FASD. Despite evidence that EGF receptors are abundantly expressed in immature neurons, including in the brain/cerebellum [79, 80], literature documenting ethanol's inhibitory effects on EGFR pathways in the developing immature brain is scant [81, 82]. Experiments using PNET2 cells demonstrated that ethanol broadly inhibits EGF-, TGF-α-, and TGF-ß-stimulated neuronal EGFR signaling, which supports cell growth, survival, metabolic function, and ASPH expression. These in vitro findings were confirmed using an established 3rd-trimester-equivalent in vivo binge alcohol exposure model because this period of development is the most susceptible to ethanol's neurotoxic effects [7]. The studies demonstrated that the binge ethanol exposures significantly reduced cerebellar EGFR tyrosine phosphorylation, PCNA, and ASPH expression. Furthermore, the ex vivo experiments showed that ethanol inhibits EGF-, TGF-α-, and TGF-ß-induced stimulation of pY-EGFR, PCNA, and ASPH in the cerebellum, consistent with results obtained using PNET2 cells. The reduced ASPH expression resulting from the downstream inhibitory effects of ethanol on EGFR signaling would, in turn, decrease immature neuronal growth and Notch pathway activation.

Together, these novel findings provide strong evidence that cerebellar neurodevelopmental impairments in FASD are mediated by inhibition of signaling through two major pathways, insulin/IGF/IRS and EGFR-Erk MAPK, both of which regulate ASPH expression. Most likely, the combined inhibitory effects of ethanol on insulin/IGF/IRS and EGFR-Erk MAPK inhibit ASPH, which in turn dysregulates Notch networks needed to support cerebellar neuron migration [83-85]. These major dual inhibitory effects of ethanol could account for the incomplete normalization of cerebellar structure and function following insulin-sensitizing interventions with dietary soy [53, 71, 86] or peroxisome proliferator-activated receptor (PPAR) agonists [57], due to sustained impairment of EGFR-related networks. Therefore, therapeutic measures designed to restore FASD-related

neurodevelopmental abnormalities must address impairments in EGFR signaling networks. Recent exploratory studies suggest that an additional/alternative therapeutic approach is to treat FASD with HE3286, which supports both the insulin/IGF and EGFR pathways and provides antioxidant protection [87-90].

Supported by AA-011431, AA028408, and AA032106 from the National Institute on Alcohol Abuse and Alcoholism of the National Institutes of Health.

REFERENCES

[1] Del Campo M, Jones KL (2017) A review of the physical features of the fetal alcohol spectrum disorders. *Eur J Med Genet* 60, 55–64.

[2] Riley EP, McGee CL (2005) Fetal alcohol spectrum disorders: an overview with emphasis on changes in brain and behavior. *Exp Biol Med (Maywood)* 230, 357–365.

[3] Roozen S, Black D, Peters GY, Kok G, Townend D, Nijhuis JG, Koek GH, Curfs LM (2016) Fetal Alcohol Spectrum Disorders (FASD): an Approach to Effective Prevention. *Curr Dev Disord Rep* 3, 229–234.

[4] Gomez DA, Abdul-Rahman OA (2021) Fetal alcohol spectrum disorders: current state of diagnosis and treatment. *Curr Opin Pediatr* 33, 570–575.

[5] Akison LK, Hayes N, Vanderpeet C, Logan J, Munn Z, Middleton P, Moritz KM, Reid N, Australian Fasd Guidelines Development Group obotAFGC (2024) Prenatal alcohol exposure and associations with physical size, dysmorphology and neurodevelopment: a systematic review and meta-analysis. *BMC Med* 22, 467.

[6] Valenzuela CF, Reid NM, Blanco BB, Carlson VL, Do AB (2025) Impact of Developmental Alcohol Exposure on the Thalamus. *Adv Exp Med Biol* 1473, 67–92.

[7] Nogales F, Jotty K, Pascual-Vaca D, Gallego-Lopez MDC, Carreras O, Ojeda ML (2025) Rat models of fetal alcohol spectrum disorders for studying the critical role of cerebellar damage: A scoping review. *Alcohol Clin Exp Res (Hoboken)* 49, 1855–1876.

[8] Granato A (2025) Defects of Cortical Microcircuits Following Early Exposure to Alcohol. *Adv Exp Med Biol* 1473, 3–13.

[9] Gao J, Liu B, Chen H, Xu P, Guo X, Yao D, Li X, Wang T, Wang Y, Yao H, Qiao S, Yuan J, Liu Y (2026) The role of DNA methylation in alcohol-mediated neurodevelopmental toxicity. *Toxicology* 519, 154315.

[10] Licheri V, Brigman JL (2021) Altering Cell-Cell Interaction in Prenatal Alcohol Exposure Models: Insight on Cell-Adhesion Molecules During Brain Development. *Front Mol Neurosci* 14, 753537.

[11] Oskera L, Charlet-Briart M, Tielens S, Nguyen L, Laguesse S (2026) Impact of Prenatal Alcohol Exposure on Cerebral Cortex Development. *Adv Exp Med Biol* 1500, 143–181.

[12] Basavarajappa BS, Subbanna S (2023) Synaptic Plasticity Abnormalities in Fetal Alcohol Spectrum Disorders. *Cells* 12.

[13] Guizzetti M, Zhang X, Goeke C, Gavin DP (2014) Glia and neurodevelopment: focus on fetal alcohol spectrum disorders. *Front Pediatr* 2, 123.

[14] Guizzetti M, Mangieri RA, Ezerskiy LA, Hashimoto JG, Bajo M, Farris SP, Homanics GE, Lasek AW, Mayfield RD, Messing RO, Roberto M (2026) Astrocytes and Alcohol Throughout the Lifespan. *Biol Psychiatry* 99, 9–20.

[15] Mathews E, Dewees K, Diaz D, Favero C (2021) White matter abnormalities in fetal alcohol spectrum disorders: Focus on axon growth and guidance. *Exp Biol Med (Maywood)* 246, 812–821.

[16] Darbinian N, Selzer ME (2022) Oligodendrocyte pathology in fetal alcohol spectrum disorders. *Neural Regen Res* 17, 497–502.

[17] Roozen S, Ehrhart F (2023) Fetal alcohol spectrum disorders and the risk of crime. *Handb Clin Neurol* 197, 197–204.

[18] Tong M, Andreani T, Krotow A, Gundogan F, de la Monte SM (2016) Potential Contributions of the Tobacco Nicotine-Derived Nitrosamine Ketone to White Matter Molecular Pathology in Fetal Alcohol Spectrum Disorder. *Int J Neurol Brain Disord* 3, 1–12.

[19] Ramsay M (2010) Genetic and epigenetic insights into fetal alcohol spectrum disorders. *Genome Med* 2, 27.

[20] de la Monte SM, Tong M, Bowling N, Moskal P (2011) si-RNA inhibition of brain insulin or insulin-like growth factor receptors causes developmental cerebellar abnormalities: relevance to fetal alcohol spectrum disorder. *Mol Brain* 4, 13.

[21] Smith SM (2025) Nonconceptus Mechanisms of Prenatal Alcohol Exposure That Disrupt Embryo-Fetal Development: An Integrative View. *Alcohol Res* 45, 07.

[22] de la Monte SM, Wands JR (2005) Review of insulin and insulin-like growth factor expression, signaling, and malfunction in the central nervous system: relevance to Alzheimer's disease. *Journal of Alzheimer's disease : JAD* 7, 45–61.

[23] de la Monte SM, Sutherland G (2025) Dual Stages of Alcohol-Related Cerebral White Matter Degeneration Reviewed: Early-Stage Stress/Neuroinflammation Versus Late-Stage Impaired Insulin/IGF Signaling Through Akt-mTOR-Review. *ASN Neuro* 17, 2573965.

[24] Yoon MS (2017) The Role of Mammalian Target of Rapamycin (mTOR) in Insulin Signaling. *Nutrients* 9, 1176.

[25] Querfurth H, Lee HK (2021) Mammalian/mechanistic target of rapamycin (mTOR) complexes in neurodegeneration. *Mol Neurodegener* 16, 44.

[26] Carter JJ, Tong M, Silbermann E, Lahousse SA, Ding FF, Longato L, Roper N, Wands JR, de la Monte SM (2008) Ethanol impaired neuronal migration is associated with reduced aspartyl-asparaginyl-beta-hydroxylase expression. *Acta Neuropathol* 116, 303–315.

[27] Gundogan F, Elwood G, Longato L, Tong M, Feijoo A, Carlson RI, Wands JR, de la Monte SM (2008) Impaired placentation in fetal alcohol syndrome. *Placenta* 29, 148–157.

[28] de la Monte SM, Tong M, Carlson RI, Carter JJ, Longato L, Silbermann E, Wands JR (2009) Ethanol inhibition of aspartyl-asparaginyl-beta-hydroxylase in fetal alcohol spectrum disorder: Potential link to the impairments in central nervous system neuronal migration. *Alcohol* 43, 225–240.

[29] Tong M, Gonzalez-Navarrete H, Kirchberg T, Gotama B, Yalcin EB, Kay J, de la Monte SM (2017) Ethanol-Induced White Matter Atrophy Is Associated with Impaired Expression of Aspartyl-Asparaginyl-beta-Hydroxylase (ASPH) and Notch Signaling in an Experimental Rat Model. *J Drug Alcohol Res* 6.

[30] Gundogan F, Tong M, M. de la Monte S (2024) Association between dietary soy prevention of fetal alcohol spectrum disorder and normalization of placental insulin and insulin-like growth

factor signaling networks and downstream effector molecule expression. *Gene & Protein in Disease* 3, 3113.

[31] Lavaissiere L, Jia S, Nishiyama M, de la Monte S, Stern AM, Wands JR, Friedman PA (1996) Overexpression of human aspartyl(asparaginyl)beta-hydroxylase in hepatocellular carcinoma and cholangiocarcinoma. *J Clin Invest* 98, 1313–1323.

[32] Ince N, de la Monte SM, Wands JR (2000) Overexpression of human aspartyl (asparaginyl) beta-hydroxylase is associated with malignant transformation. *Cancer Res* 60, 1261–1266.

[33] Sepe PS, Lahousse SA, Gemelli B, Chang H, Maeda T, Wands JR, de la Monte SM (2002) Role of the aspartyl-asparaginyl-beta-hydroxylase gene in neuroblastoma cell motility. *Lab Invest* 82, 881–891.

[34] Maeda T, Sepe P, Lahousse S, Tamaki S, Enjoji M, Wands JR, de la Monte SM (2003) Antisense oligodeoxynucleotides directed against aspartyl (asparaginyl) beta-hydroxylase suppress migration of cholangiocarcinoma cells. *J Hepatol* 38, 615–622.

[35] Silbermann E, Moskal P, Bowling N, Tong M, de la Monte SM (2010) Role of aspartyl-(asparaginyl)-beta-hydroxylase mediated notch signaling in cerebellar development and function. *Behav Brain Funct* 6, 68.

[36] Cantarini MC, de la Monte SM, Pang M, Tong M, D'Errico A, Trevisani F, Wands JR (2006) Aspartyl-asparagyl beta hydroxylase over-expression in human hepatoma is linked to activation of insulin-like growth factor and notch signaling mechanisms. *Hepatology* 44, 446–457.

[37] Jia S, VanDusen WJ, Diehl RE, Kohl NE, Dixon Ra, Elliston KO, Stern aM, Friedman Pa (1992) cDNA cloning and expression of bovine aspartyl (asparaginyl) beta-hydroxylase. *J Biol Chem* 267, 14322–14327.

[38] Lawton M, Tong M, Gundogan F, Wands JR, de la Monte SM (2010) Aspartyl-(asparaginyl) beta-hydroxylase, hypoxia-inducible factor-alpha and Notch cross-talk in regulating neuronal motility. *Oxidative medicine and cellular longevity* 3, 347–356.

[39] Borgas DL, Gao JS, Tong M, Roper N, de la Monte SM (2015) Regulation of Aspartyl-(Asparaginyl)-beta-Hydroxylase Protein Expression and Function by Phosphorylation in Hepatocellular Carcinoma Cells. *J Nat Sci* 1.

[40] Borgas DL, Gao JS, Tong M, de la Monte SM (2015) Potential Role of Phosphorylation as a Regulator of Aspartyl-(asparaginyl)-beta-hydroxylase: Relevance to Infiltrative Spread of Human Hepatocellular Carcinoma. *Liver Cancer* 4, 139–153.

[41] Fife M, Tong M, Das B, Rodriguez R, Chokkalingam P, Carlson RI, de la Monte SM (2025) Chondrosarcoma: Multi-Targeting Therapeutic Effects of Doxorubicin, BEZ235, and the Small Molecule Aspartyl-Asparaginyl-beta-hydroxylase Inhibitor SMI1182. *Cancers (Basel)* 17, 1671.

[42] Estrada C, Villalobo A (2006) Epidermal Growth Factor Receptor in the Adult Brain. In *The Cell Cycle in the Central Nervous System*, Janigro D, ed. Humana Press Inc, Totowa, NJ, pp. 265–277.

[43] Tito C, Masciarelli S, Colotti G, Fazi F (2025) EGF receptor in organ development, tissue homeostasis and regeneration. *J Biomed Sci* 32, 24.

[44] Xian CJ, Zhou XF (1999) Roles of transforming growth factor-alpha and related molecules in the nervous system. *Mol Neurobiol* 20, 157–183.

[45] Sadeghzadeh S, Ebrahimi R, Zareiye A, Meshkin A, Aghabozorgi R, Lotfi M, Ghanbari F, Shahcheraghi SH, Aghili ZS (2025) Targeting TGF-beta signaling in glioblastoma: therapeutic implications and novel drug development strategies. *Brain Tumor Pathol* 42, 105–120.

[46] Kaminska B, Wesolowska A, Danilkiewicz M (2005) TGF beta signalling and its role in tumour pathogenesis. *Acta Biochim Pol* 52, 329–337.

[47] Romano R, Bucci C (2020) Role of EGFR in the Nervous System. *Cells* 9, 1887.

[48] Dinchuk JE, Henderson NL, Burn TC, Huber R, Ho SP, Link J, O'Neil KT, Focht RJ, Scully MS, Hollis JM, Hollis GF, Friedman PA (2000) Aspartyl beta -hydroxylase (Asph) and an evolutionarily conserved isoform of Asph missing the catalytic domain share exons with junctin. *J Biol Chem* 275, 39543–39554.

[49] Chung W, Kim M, de la Monte S, Longato L, Carlson R, Slagle BL, Dong X, Wands JR (2016) Activation of signal transduction pathways during hepatic oncogenesis. *Cancer Lett* 370, 1–9.

[50] Dong X, Lin Q, Aihara A, Li Y, Huang CK, Chung W, Tang Q, Chen X, Carlson R, Nadolny C, Gabriel G, Olsen M, Wands JR (2015) Aspartate beta-Hydroxylase expression promotes a malignant pancreatic cellular phenotype. *Oncotarget* 6, 1231–1248.

[51] Sturla LM, Tong M, Hebda N, Gao J, Thomas JM, Olsen M, de la Monte SM (2016) Aspartate-beta-hydroxylase (ASPH): A potential therapeutic target in human malignant gliomas. *Heliyon* 2, e00203.

[52] Andreani T, Tong M, Gundogan F, Silbermann E, de la Monte SM (2016) Differential Effects of 3rd Trimester-Equivalent Binge Ethanol and Tobacco-Specific Nitrosamine Ketone Exposures on Brain Insulin Signaling in Adolescence. *J Diabetes Relat Disord* 1, 105–114.

[53] de la Monte SM, Tong M, Delikkaya B (2023) Differential Early Mechanistic Frontal Lobe Responses to Choline Chloride and Soy Isoflavones in an Experimental Model of Fetal Alcohol Spectrum Disorder. *Int J Mol Sci* 24, 7595.

[54] de la Monte SM, Ganju N, Banerjee K, Brown NV, Luong T, Wands JR (2000) Partial rescue of ethanol-induced neuronal apoptosis by growth factor activation of phosphoinositol-3-kinase. *Alcohol Clin Exp Res* 24, 716–726.

[55] Feoktistova M, Geserick P, Leverkus M (2016) Crystal Violet Assay for Determining Viability of Cultured Cells. *Cold Spring Harb Protoc* 2016, pdb prot087379.

[56] Stern-Straeter J, Bonaterra GA, Hormann K, Kinscherf R, Goessler UR (2009) Identification of valid reference genes during the differentiation of human myoblasts. *BMC Mol Biol* 10, 66.

[57] Le T, Tong M, Nguyen V, de la Monte SM (2013) PPAR Agonist Rescue of Ethanol-Impaired Brain Insulin Signaling: Cerebellar Slice Culture Model. *Journal of Drug and Alcohol Research* 2, 1–9.

[58] Shaughness M, Acs D, Brabazon F, Hockenbury N, Byrnes KR (2020) Role of Insulin in Neurotrauma and Neurodegeneration: A Review. *Front Neurosci* 14, 547175.

[59] McGinnis K, Ku GM, VanDusen WJ, Fu J, Garsky V, Stern aM, Friedman Pa (1996) Site-directed mutagenesis of residues in a conserved region of bovine aspartyl (asparaginyl) beta-hydroxylase: evidence that histidine 675 has a role in binding Fe2+. *Biochemistry* 35, 3957–3962.

[60] Tong M, Gao JS, Borgas D, de la Monte SM (2013) Phosphorylation Modulates Aspartyl-(Asparaginyl)-beta Hydroxylase Protein Expression, Catalytic Activity and Migration in Human Immature Neuronal Cerebellar Cells. *Cell Biol (Henderson, NV)* 6.

[61] de la Monte SM, Tamaki S, Cantarini MC, Ince N, Wiedmann M, Carter JJ, Lahousse SA, Califano S, Maeda T, Ueno T, D'Errico A, Trevisani F, Wands JR (2006) Aspartyl-(asparaginyl)-beta-hydroxylase regulates hepatocellular carcinoma invasiveness. *J Hepatol* 44, 971–983.

[62] Lahousse SA, Carter JJ, Xu XJ, Wands JR, de la Monte SM (2006) Differential growth factor regulation of aspartyl-(asparaginyl)-beta-hydroxylase family genes in SH-Sy5y human neuroblastoma cells. *BMC Cell Biol* 7, 41.

[63] de la Monte SM, Wands JR (2010) Role of central nervous system insulin resistance in fetal alcohol spectrum disorders. *J Popul Ther Clin Pharmacol* 17, e390–404.

[64] Son AI, Mohammad S, Sasaki T, Ishii S, Yamashita S, Hashimoto-Torii K, Torii M (2020) Dual Role of Rbpj in the Maintenance of Neural Progenitor Cells and Neuronal Migration in Cortical Development. *Cereb Cortex* 30, 6444–6457.

[65] Wiszniak S, Schwarz Q (2019) Notch signalling defines dorsal root ganglia neuroglial fate choice during early neural crest cell migration. *BMC Neurosci* 20, 21.

[66] Yang Z, Li PF, Chen RC, Wang J, Wang S, Shen Y, Wu X, Fang B, Cheng X, Xiong ZQ (2017) ADAM10-Initiated Release of Notch Intracellular Domain Regulates Microtubule Stability and Radial Migration of Cortical Neurons. *Cereb Cortex* 27, 919–932.

[67] Aujla PK, Bora A, Monahan P, Sweedler JV, Raetzman LT (2011) The Notch effector gene Hes1 regulates migration of hypothalamic neurons, neuropeptide content and axon targeting to the pituitary. *Dev Biol* 353, 61–71.

[68] de la Monte SM, Elgas E, Tong M, Delikkaya B, Yang Y (2023) Differential rescue effects of choline chloride and soy isolate on metabolic dysfunction in immature central nervous system neurons: Relevance to fetal alcohol spectrum disorder. *Diabetes Manag* 13, 107–118.

[69] Zabala V, Silbermann E, Re E, Andreani T, Tong M, Ramirez T, Gundogan F, de la Monte SM (2016) Potential Co-Factor Role of Tobacco Specific Nitrosamine Exposures in the Pathogenesis of Fetal Alcohol Spectrum Disorder. *Gynecol Obstet Res* 2, 112–125.

[70] Leung ECH, Jain P, Michealson MA, Choi H, Ellsworth-Kopkowski A, Valenzuela CF (2024) Recent breakthroughs in understanding the cerebellum's role in fetal alcohol spectrum disorder: A systematic review. *Alcohol* 119, 37–71.

[71] de la Monte SM, Tong M, Ziplow J, Mark P, Van S, Nguyen VA (2025) Impact of Prenatal Dietary Soy on Cerebellar Neurodevelopment and Function in Experimental Fetal Alcohol Spectrum Disorder. *Nutrients* 17, 812.

[72] Halder S, Basu S, Lall SP, Ganti AK, Batra SK, Seshacharyulu P (2023) Targeting the EGFR signaling pathway in cancer therapy: What's new in 2023? *Expert Opin Ther Targets* 27, 305–324.

[73] Du Y, Karatekin F, Wang WK, Hong W, Boopathy GTK (2025) Cracking the EGFR code: Cancer biology, resistance mechanisms, and future therapeutic frontiers. *Pharmacol Rev* 77, 100076.

[74] Purow BW, Sundaresan TK, Burdick MJ, Kefas BA, Comeau LD, Hawkinson MP, Su Q, Kotliarov Y, Lee J, Zhang W, Fine HA (2008) Notch-1 regulates transcription of the epidermal growth factor receptor through p53. *Carcinogenesis* 29, 918–925.

[75] Hu T, Li C (2010) Convergence between Wnt-beta-catenin and EGFR signaling in cancer. *Mol Cancer* 9, 236.

[76] Tripurani SK, Wang Y, Fan YX, Rahimi M, Wong L, Lee MH, Starost MF, Rubin JS, Johnson GR (2018) Suppression of Wnt/beta-catenin signaling by EGF receptor is required for hair follicle development. *Mol Biol Cell* 29, 2784–2799.

[77] Luu M, Sabo E, de la Monte SM, Greaves W, Wang J, Tavares R, Simao L, Wands JR, Resnick MB, Wang L (2009) Prognostic value of aspartyl (asparaginyl)-beta-hydroxylase/humbug expression in non-small cell lung carcinoma. *Human pathology* 40, 639–644.

[78] Wang J, de la Monte SM, Sabo E, Kethu S, Tavares R, Branda M, Simao L, Wands JR, Resnick MB (2007) Prognostic value of humbug gene overexpression in stage II colon cancer. *Human pathology* 38, 17–25.

[79] Kato M, Mizuguchi M, Takashima S (1995) Developmental changes of epidermal growth factor-like immunoreactivity in the human fetal brain. *J Neurosci Res* 42, 486–492.

[80] Kornblum HI, Hussain RJ, Bronstein JM, Gall CM, Lee DC, Seroogy KB (1997) Prenatal ontogeny of the epidermal growth factor receptor and its ligand, transforming growth factor alpha, in the rat brain. *J Comp Neurol* 380, 243–261.

[81] Hamada K, Lasek AW (2020) Receptor Tyrosine Kinases as Therapeutic Targets for Alcohol Use Disorder. *Neurotherapeutics* 17, 4–16.

[82] Zhou FC, Zhao Q, Liu Y, Goodlett CR, Liang T, McClintick JN, Edenberg HJ, Li L (2011) Alteration of gene expression by alcohol exposure at early neurulation. *BMC Genomics* 12, 124.

[83] Irvin DK, Zurcher SD, Nguyen T, Weinmaster G, Kornblum HI (2001) Expression patterns of Notch1, Notch2, and Notch3 suggest multiple functional roles for the Notch-DSL signaling system during brain development. *J Comp Neurol* 436, 167–181.

[84] Weller M, Krautler N, Mantei N, Suter U, Taylor V (2006) Jagged1 ablation results in cerebellar granule cell migration defects and depletion of Bergmann glia. *Dev Neurosci* 28, 70–80.

[85] Gaiano N (2008) Strange bedfellows: Reelin and Notch signaling interact to regulate cell migration in the developing neocortex. *Neuron* 60, 189–191.

[86] de la Monte SM, Tong M, Ziplow J, Mark P, Van S, Nguyen VA (2025) Dietary Soy Preserves Cognitive Function in Experimental Fetal Alcohol Spectrum Disorder: Role of Increased Signaling through Notch and Gonadotropin Releasing Hormone Networks. *J Behav Brain Sci* 15, 11–46.

[87] Reading CL, Flores-Riveros J, Stickney DR, Frincke JM (2013) An anti-inflammatory sterol decreases obesity-related inflammation-induced insulin resistance and metabolic dysregulation. *Mediators Inflamm* 2013, 814989.

[88] Reading CL, Frincke JM, White SK (2012) Molecular targets for 17alpha-ethynyl-5-androstene-3beta,7beta,17beta-triol, an anti-inflammatory agent derived from the human metabolome. *PLoS One* 7, e32147.

[89] Reading CL, Stickney DR, Flores-Riveros J, Destiche DA, Ahlem CN, Cefalu WT, Frincke JM (2013) A synthetic anti-inflammatory sterol improves insulin sensitivity in insulin-resistant obese impaired glucose tolerance subjects. *Obesity (Silver Spring)* 21, E343–349.

[90] Wang T, Villegas S, Huang Y, White SK, Ahlem C, Lu M, Olefsky JM, Reading C, Frincke JM, Alleva D, Flores-Riveros J (2010) Amelioration of glucose intolerance by the synthetic androstene HE3286: link to inflammatory pathways. *The Journal of pharmacology and experimental therapeutics* 333, 70–80.